

K-25

OAK RIDGE K-25 SITE

MARTIN MARIETTA

Corrosion Monitoring in the UF₆ Cylinder Yards at the Oak Ridge K-25 Site: FY 1994 Report

Mukund Rao
Ron Adamski
Jeff Broders
Alvin Ellis
David Freels
Don Kelley
Bonnie Phillips

October 1994

This document has been approved for release
to the public by:

Asst. David B. Hilliland 11/30/94
Technical Information Officer Date
Oak Ridge K-25 Site

MANAGED BY
MARTIN MARIETTA ENERGY SYSTEMS, INC.
FOR THE UNITED STATES
DEPARTMENT OF ENERGY

DISTRIBUTION OF THIS DOCUMENT IS UNLIMITED

DISCLAIMER

This report was prepared as an account of work sponsored by an agency of the United States Government. Neither the United States Government nor any agency thereof, nor any of their employees, makes any warranty, express or implied, or assumes any legal liability of responsibility for the accuracy, completeness, or usefulness of any information, apparatus, product, or process disclosed, or represents that its use would not infringe privately owned rights. Reference herein to any specific commercial product, process, or service by trade name, trademark, manufacturer, or otherwise, does not necessarily constitute or imply its endorsement, recommendation, or favoring by the United States Government or any agency thereof. The views and opinions of authors expressed herein do not necessarily state or reflect those of the United States Government or any agency thereof.

This report has been reproduced directly from the best available copy.

Available to DOE and DOE contractors from the Office of Scientific and Technical Information, P.O. Box 62, Oak Ridge, TN 37831; prices available from (615) 576-8401.

Available to the public from the National Technical Information Service, U.S. Department of Commerce, 5285 Port Royal Rd., Springfield, VA 22161.
NTIS price codes—Printed Copy: ____ Microfiche A01

NOTICE: This document contains information of a preliminary nature. It is subject to revision or correction and therefore does not represent a final report.

DISCLAIMER

Portions of this document may be illegible in electronic image products. Images are produced from the best available original document.

**Corrosion Monitoring in the
UF₆ Cylinder Yards at the
Oak Ridge K-25 Site:
FY 1994 Report**

Prepared by
Mukund Rao
Midwest Technical Inc.
Oak Ridge, Tennessee 37831
under subcontract 1BK-02268C with
Martin Marietta Energy Systems, Inc.

and

Ron Adamski
Jeff Broders
Alvin Ellis
David Freels
Don Kelley
Bonnie Phillips
K-25 Site Technical Division
OAK RIDGE K-25 SITE
Oak Ridge, Tennessee 37831

October 1994

MARTIN MARIETTA ENERGY SYSTEMS, INC.
managing the

Environmental Restoration and Waste Management Programs at

Oak Ridge K-25 Site
Oak Ridge National Laboratory
Oak Ridge Y-12 Plant
under Contract DE-AC05-84OR21400

Paducah Gaseous Diffusion Plant
Portsmouth Gaseous Diffusion Plant
under Contract DE-AC05-76OR00001

for the
U.S. DEPARTMENT OF ENERGY

MASTER

DISTRIBUTION OF THIS DOCUMENT IS UNLIMITED

TABLE OF CONTENTS

ACKNOWLEDGEMENTS	v
LIST OF FIGURES	vii
LIST OF TABLES	ix
ACRONYMS	xi
EXECUTIVE SUMMARY	xiii
ABSTRACT	xv
1. INTRODUCTION	1
2. EXPERIMENTAL PROCEDURES	3
3. RESULTS	11
4. DISCUSSION	31
5. ONGOING AND FUTURE WORK	35
6. SUMMARY	39
REFERENCES	41
APPENDIX A	43

ACKNOWLEDGEMENTS

This work was funded as part of the U.S. Department of Energy's Uranium Hexafluoride (UF₆) Cylinders Program at Martin Marietta Energy Systems, Inc., Valerie Newman, Program Manager. The corrosion monitoring program was initiated in the Technical Division at the Oak Ridge K-25 Site by Helen Henson. The ultrasonic thickness data were provided by Halen Philpot, K-25 Site UF₆ Cylinders Program Manager. Significant historical input and guidance were provided by Curtis Barlow and Ken Ziehlke.

LIST OF FIGURES

1	Typical stacking arrangement of UF ₆ cylinders in the storage yards at the Oak Ridge K-25 Site	4
2	(a) and (b) Examples of heavy corrosion scale and pitted surfaces seen on UF ₆ cylinders at the Oak Ridge K-25 Site	5
3	Cylinder instrumented with TOW sensors, thermocouples and corrosion probes on stainless steel bands and 1-sided corrosion coupons attached to cylinder surfaces with magnets	9
4	Percent wetness measured in (a) top row, top positions and (b) bottom row, bottom positions	14
5	(a) and (b) Wetness data from top row, top and bottom row, bottom sensors along with rainfall data collected during two time periods in April, 1994 at the K-yard south location	15
6	Surface temperature data from TR,T and BR, B surfaces at K-yard south for the same time period as Fig. 5(a) showing much greater temperature fluctuations on TR,T surfaces due to radiative heating and cooling	16
7	(a) and (b) Rainfall data and periods when TR, T and BR, B TOW sensors were "on" during December 1993 and January 1994 at the E-yard location	18
8	Relative humidity and corresponding time-of-wetness sensor responses from E-yard for the months of (a) February 1993 and (b) April 1993	19
9	Typical corrosion probe data, for Probes 1-4 mounted on cylinders at the K-yard north location	20
10	(a) Corrosion probe data from probes installed in various orientations on the coupon rack in K-yard	21
11	Corrosion rates calculated from data from corrosion probes	23
12	Corroding elements of Probes 1 and 2 after 158 days of exposure	24
13	Corroding elements of Probes 1 and 2 after 500 days of exposure	25
14	Data from corrosion probes mounted outside the laboratory area	26
15	Photographs of (a) Probe 54 (mounted facing up horizontally) and (b) Probe 56 (mounted facing up inclined at 45°) after a period of rain	27

16	Data from Probe 54 (mounted facing up horizontally) showing relationship between probe readings and periods of precipitation	28
17	Corrosion rates measured after 1- and 2-year exposures from ASTM G50 type coupons mounted on coupon racks in E-yard and K-yard	29
18	Corrosion rates measured after 1-year exposure from coupons mounted on cylinders in K-yard	29
19	Corrosion rates measured after 6-month exposure from coupons in ground contact in E and K yards	30
20	Results of pit depth measurements on cylinder coupons after 1-year exposure showing deeper pits on top facing coupons	31
A1	Data from corrosion probes 1-4 (on cylinders) and 50-53 (between top row cylinders) at the K-yard North location	45
A2	Data from corrosion probes 7-12 (on cylinders) and 42-45 (between top row cylinders) at the K-yard South location	46
A3	Data from corrosion probes 13-16 on cylinders at the E-yard location	47
A4	Data from corrosion probes 17 and 18 on a new cylinder at the entrance to E-yard	47
A5	Data from corrosion probes 19-22 on relatively heavily corroded TR and BR cylinders in K yard, row 10, concrete pad	48
A6	Data from corrosion probes 25 and 26 on a relatively lightly corroded BR cylinder in K yard, row 14, gravel pad	48
A7	Data from corrosion probes 24, 27-31 (on cylinders) and 46-49 (between top row cylinders) on relatively lightly corroded cylinders in K-yard, row 4, concrete pad	49
A8	Data from corrosion probes 5, 6, 23, and 33 on relatively heavily corroded TR and BR cylinders in K-yard, row 3, concrete pad	50

LIST OF TABLES

1	Deployment details of atmospheric corrosion probes	7
2	Typical time-of-wetness (TOW) data, gathered over an 8-hour period in E-yard	12
3	Monthly data from the three time-of-wetness sensor sets	13
4	Published observations of atmospheric corrosion behavior as related to length of exposure	36

ACRONYMS

ANSI	American National Standards Institute
ASME	American Society of Mechanical Engineers
ASTM	American Society for Testing and Materials
DOE	U.S. Department of Energy
HF	hydrofluoric acid
TOW	time-of-wetness
UF ₆	uranium hexafluoride

EXECUTIVE SUMMARY

An atmospheric corrosion monitoring program using time-of-wetness (TOW) instrumentation, corrosion probes, and corrosion coupons has been ongoing at the U.S. Department of Energy's Oak Ridge K-25 Site repository of uranium hexafluoride (UF₆) cylinders. Data from these measurements have been providing significant information on the onset and progress of corrosion of the UF₆ cylinders.

Results from TOW sensors and corrosion probes are in good agreement but do not completely agree with early data from the corrosion coupons. There appears to be no significant effect derived from cylinder yard, row, or stacking position, although early data from the corrosion coupons show possible yard and stacking differences. However, it is too soon to form conclusions. Potential differences may not be observed in the corrosion probes and TOW sensors due to differences in individual sensor responses. Sensor calibration is currently under way.

Corrosion loss time curves from corrosion probes were generally similar, irrespective of when they were initially exposed, indicating no strong seasonal effects. However, several probes show a slowdown/acceleration of corrosion rates over discrete time periods. This behavior is being examined and may be due to a combination of seasonal effects, probe characteristics, and chemistry of the rust layers. Corrosion rates are initially significantly higher on cylinder tops (top-facing, open probes) than bottoms (protected surfaces).

This is apparently related to greater wetting of such surfaces from condensation, which was rarely observed on protected surfaces (cylinder bottoms). In addition, wetting of cylinder bottoms occurred only during heavy or very frequent rain, in which case the wetted bottoms tended to stay wet longer than the cylinder tops. Shelter or protection appears to mainly delay the onset of corrosion by keeping surfaces dry, and corrosion rates on such surfaces increase once a corrosion product forms. However, results are currently insufficient to establish any final long-term differences in corrosion rates between sheltered and open exposures.

The probes and TOW data do not agree with ultrasonic measurements, which have shown greater thinning and pitting on cylinder bottoms in K-yard. This observation may be related to damage caused by prior storage in which the cylinder bottoms may have been in contact with the ground, leading to severe corrosion. Data from the monitoring program at Paducah also appear to directly contradict the K-25 Site results, and these possible site-to-site differences are being examined. Other planned future work includes the analysis of corrosion identification, characterization and monitoring of localized corrosion effects (including galvanic and crevice corrosion), products and their effects on subsequent corrosion and the development of a predictive corrosion model.

ABSTRACT

Depleted uranium hexafluoride (UF_6) at the U.S. Department of Energy's K-25 Site at Oak Ridge, Tennessee, has been stored in large steel cylinders that have undergone significant atmospheric corrosion damage over the last 35 years. A detailed experimental program to characterize the corrosion damage was initiated in 1992.

Large amounts of corrosion scale and deep pits are found to cover UF_6 cylinder surfaces. Ultrasonic wall thickness measurements have shown uniform corrosion losses up to 20 mils (0.5 mm) and pits up to 100 mils (2.5 mm) deep. Electrical resistance corrosion probes, TOW sensors, and thermocouples have been attached to cylinder bodies. Atmospheric conditions are monitored using rain gauges, relative humidity sensors, and thermocouples. Long-term (16-year) data are being obtained from mild steel corrosion coupons on test racks as well as attached directly to cylinder surfaces. Corrosion rates have been found to be intimately related to the times-of-wetness, both tending to be higher on cylinder tops due to apparent sheltering effects. Data from the various tests are compared, discrepancies are discussed, and a pattern of cylinder corrosion as a function of cylinder position and location is described.

1. INTRODUCTION

The U.S. Department of Energy's (DOE's) K-25 Site at Oak Ridge, Tennessee, produced enriched uranium using the gaseous diffusion process until it was permanently shut down in 1987. Depleted uranium hexafluoride (UF_6) from the process has been stored at the site in 10- and 14-ton mild steel [American Society for Testing and Materials (ASTM) grades A285 and A516] cylinders stacked in outdoor yards. The UF_6 cylinders typically are 4 ft in diameter and 10 to 12 ft long with wall thicknesses of 5/16 in. (8 mm), and are designed, manufactured and maintained in accordance with the American Society of Mechanical Engineers (ASME) Boiler and Pressure Vessel Code for unfired pressure vessels. A large portion of the approximately 5000 such cylinders, some of which have been in storage for up to 35 years, have undergone significant atmospheric corrosion damage during storage. Since the cylinders are expected to remain in outdoor storage for at least another 25 years, there is a potential for cylinder wall failures leading to releases of UF_6 and associated formation of toxic hydrofluoric acid (HF). American National Standards Institute (ANSI) N14.1 specifies that wall thicknesses of nominally 5/16-in. thick cylinders do not fall below 1/4 in. (6.4 mm).

Cylinders were initially coated with a zinc chromate primer and an enamel topcoat, but most of these coatings have weathered away since they were not designed for long-term outdoor storage. Cylinders are typically covered with thick corrosion scale, large pieces of which have spalled off the sides and bottoms. Surfaces are covered with deep pits, and areas have developed a "rock candy" appearance. Spot measurements using ultrasonic thickness gauges have shown uniform wall thinning on the order of 20 mils (0.5 mm) and pits up to 100 mils (2.5 mm) deep, indicating that a significant number of cylinders may have areas that have thinned down below ANSI N14.1 limits.

Early monitoring mainly involved visual inspection and documentation of corrosion damage and evaluation of potential monitoring techniques.¹⁻³ A formal corrosion monitoring program of this nature was put in place in FY88, and included the initiation of a program placing corrosion coupons on racks in the cylinder yards starting in 1991.¹ Screening of electrical resistance corrosion probes for corrosion rate measurements was also initiated, but corrosion probes were not incorporated into the monitoring program until FY93.

It is well known that the extent of corrosive attack on structures exposed to the atmosphere varies with the micro-climate around the structure as well as with the nature of exposure of individual areas of the structure.⁴⁻¹⁸ Factors influencing corrosion, such as TOW and the constituents of the immediate environment, are in turn affected by the nature of the exposed surface, drainage, and humidity factors. A wide range of corrosion behavior may therefore be expected. A wide variety of cylinder damage has been observed, but the distribution of damage and number of cylinders in need of corrective action of some sort is unknown at this time. In 1992, a detailed experimental program was initiated to characterize and monitor the atmospheric corrosion damage of the cylinders and provide guidelines for corrective actions.

2. EXPERIMENTAL PROCEDURES

Three main experimental projects describe the corrosion monitoring program as it stood in FY94: TOW monitoring, corrosion monitoring with electrical resistance corrosion probes, and corrosion monitoring with corrosion coupons. Data from these are supplemented with ultrasonic wall thickness measurements that yield quantitative data on cylinder wall thinning.

Most of the UF₆ cylinders are stored in two unprotected yards, designated as E-yard and K-yard. The UF₆ cylinders are stacked in two-high rows, with the bottom row of cylinders supported on contoured wooden saddles and the top row of cylinders resting in the valleys between the bottom row of cylinders. The wooden saddles are designed to keep the bottoms of cylinders 4 in. off the ground. Top- or bottom-row cylinders are typically spaced a few inches apart within a row (although they are often in contact), and cylinder rows are typically a few feet apart, allowing access for inspection and maintenance. The surface of E-yard is concrete; the surface of K-yard is part concrete and part compacted gravel. The concrete surface of E-yard is relatively even and intact, with good drainage of rainwater, whereas the concrete in K-yard is buckled and broken in several areas, leading to uneven drainage and water pooling. In some of these areas, cylinders have sunk into contact with the ground. The compacted gravel area is relatively well drained. Figure 1 shows a typical stacking arrangement of cylinders on the concrete pad in K-yard. Figure 2 shows examples of heavy corrosion scale and pitted surfaces on cylinders.

Based on these cylinder yard conditions, three primary locations were chosen for instrumentation—one in E-yard and one each in the broken concrete (K-South) and compacted gravel (K-North) areas of K-yard. A bottom-row cylinder and one of the top-row cylinders resting on it were instrumented at each location. To ease installation, the sensors were pre-mounted on 3-in.-wide, 25-mil-thick stainless steel bands/straps using a strain gauge mounting epoxy mixed with copper powder to improve the thermal conductivity between the sensor and the mounting surface. As protection, a coating of a silicone-based adhesive was applied over the encapsulated surfaces, taking care to keep the active sensor elements clear. Lead wires were attached to the sensors after they had been mounted, and the wires and soldered junctions were also covered with a protective layer of silicone-based adhesive. The bands were cinched tightly around the cylinders. Each band had two sets of sensors, so that one set would be located on the top surface and the other on the bottom surface of the cylinder to which the band was attached. This arrangement allowed corrosion monitoring as functions of cylinder position as well as location on the cylinder surface. Each of the three primary cylinder locations therefore had four sensor sets, distributed two each on a top-row and a bottom-row cylinder. Separate bands, mounted adjacent to each other, were used for the TOW and corrosion probe sensor sets.

Each TOW instrumentation set consists of a TOW sensor and a thermocouple mounted adjacent to each other. The TOW sensor is a resistance-type of copper grid. Moisture condensing on the sensor creates a short-circuit and thus a measurable change in the electrical resistance of the grid. The sensors are available in two sizes—a roughly 1-in. square configuration similar in size to Sereda-type ASTM bimetallic sensors^{10,11} and a larger 2-in. square sensor. The larger sensors were selected because these sensors will be more robust and less likely to give erroneous results due to contamination, dirt, and similar factors. Sereda-type copper-gold bimetallic sensors were also attached to the straps but have not been used. In addition to the sensors mounted on the straps, each of the three primary locations also has a weatherhead located at ground level and a second weatherhead located beneath the top-row cylinder. The weatherheads are equipped with a relative



Fig. 1. Typical stacking arrangement of UF_6 cylinders in the storage yards at the Oak

humidity sensor and a solid-state temperature sensor for ambient temperature measurements. A rain gauge is also installed at each location. Data from the sensors/gauges are downloaded every 10 minutes into a datalogger. A total of 12 TOW sensors have been deployed among the three cylinder locations described above.

Electrical resistance corrosion probes work on the principle that corrosion loss causes a decrease in cross-sectional area of the metal sensor, which in turn leads to an increase in the electrical resistance. In a corrosion probe, the change in resistance of an exposed test element is balanced against the (constant) resistance of a similar reference element that is protected against corrosion. The corrosion probes used were atmospheric corrosion probes obtained from Rohrback Cosasco Systems, Santa Fe Springs, California. The plain flat, 8-mil-thick carbon steel probe elements are mounted on a fiberglass backing with further fiberglass encapsulation of the reference element. The carbon steel is a good approximation to the A-285 and A-516 steels used in UF_6 cylinder construction. The approximate overall dimensions of the probe are 3 in. long \times 1 in. wide \times 1/16 in. thick. The electrical resistance of the probes was monitored using a Model IN-8000 E/R Portable Electrical Resistance Monitor from Cortest Instrument Systems, Willoughby, Ohio. Good correlation has been found in field studies comparing atmospheric corrosion of electrical resistance corrosion probes and conventional weight loss coupons.¹² Initial probe readings were recorded at the time of deployment, after which the probes were typically monitored at 1- or 2-week intervals. A

record of temperature and weather conditions was also made at each reading, supplemented by data from the TOW weatherheads.

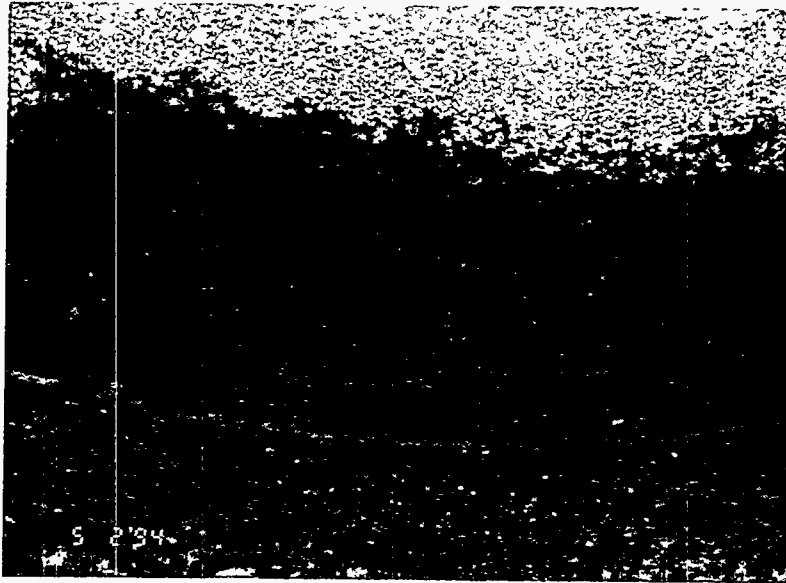
A total of 56 corrosion probes were deployed between February 1993 and January 1994, 12 of which were in conjunction with TOW sensors, as described above. The remaining probes have been distributed in several areas, including on corrosion coupon racks, in the laboratory area and at strategic cylinder locations including in cylinder skirts and between cylinders. Many of these are oriented facing the sky or ground and in a sheltered or open position. Table 1 summarizes the details of deployment.

Field exposure tests with corrosion coupons are also being conducted. Sets of 4-in. × 6-in. coupons of A285, A516 and A36 steels have been deployed at orientations of 0° and 30° to the horizon on south-facing coupon racks in E-yard and K-yard ("ASTM coupons"). Scheduled retrievals of four replicates are at 1-, 2-, 4-, 8- and 16-year intervals following ASTM G50 guidelines.¹³ After retrieval, mass losses and corrosion rates are measured after dissolving the corrosion products in a solution of 0.5 g/L sodium lauryl sulfate, 100 mL/L concentrated hydrochloric acid and 125 g/L sodium hypophosphite. Coupons have been exposed starting in March 1991, and data from 1- and 2-year exposures have been collected to date.

In addition to coupon rack exposures, sets of A516 steel coupons were mounted directly on cylinder surfaces in May 1993 ("supplemental coupons" or "cylinder coupons") to monitor differences in local corrosivities. To restrict corrosion to only one exposed face, the A516 coupons were attached to mild steel coupons with double-sided adhesive tape.¹⁴ The mild steel side of the combination was then attached to cylinder surfaces using small neodymium-iron-boron magnets, leaving the A516 side exposed. After exposure, the two pieces are separated and corrosion rates estimated after removing the corrosion products from the single exposed face of each coupon. Sets of coupons (three replicates) have been deployed for 1-, 2-, 4-, 8-, and 16-year exposures on the K-yard coupon rack and on five groups of cylinders, including the three cylinder groups with TOW and corrosion probe instrumentation. In each cylinder group, the coupons have been placed on top of the top-row cylinder and on the top and bottom of the bottom-row cylinder. (No coupons were attached to the bottom of the top row cylinders.) To date, data from 1-year exposures have been collected. Additional coupons have been recently (October 1993) exposed in ground contact next to cylinders at the various locations, to estimate effects of direct cylinder contact with the ground. The ground-contact coupons include both one-sided (sky-facing surfaces protected) and two-sided (sky-facing surfaces exposed) coupons.

Figure 3 shows a cylinder instrumented with stainless steel straps containing TOW sensors, thermocouples, and corrosion probes. A few of the cylinder coupons can also be seen in the background.

The cylinders are visually inspected routinely, and supplemental information is obtained from these inspections. In addition, a parallel inspection program has been measuring cylinder wall thicknesses using ultrasonic thickness gauges, and an automated ultrasonic scanning system capable of traversing the circumference of a cylinder has been recently obtained. These data provide a good measure of actual metal loss around the cylinders due to both uniform and pitting corrosion, and some of these results are discussed for comparison with the corrosion monitoring studies.



(a)



(b)

Fig. 2. (a) and (b) Examples of heavy corrosion scale and pitted surfaces seen on UF_6 cylinders at the Oak Ridge K-25 Site.

Table 1. Deployment details of atmospheric corrosion probes

Probe No.	Start Date	Yard	Row	Cylinder No., Probe Location	Comments
1	3/29/93	K	14 (gravel) (K-North)	18329, TR, T	With TOW instrumentation and corrosion coupons
2	3/29/93			18329, TR, B	
3	3/29/93			12137, BR, T	
4	3/29/93			12137, BR, B	
50	10/28/93			12137/18346, BC	Facing up, open
51	10/28/93			12137/18346, BC	Facing down, open
52	10/28/93			12137/18346, BC	Facing down, sheltered
53	10/28/93			12137/18346, BC	Facing up, sheltered
7	3/30/93			K	4 (broken concrete) (K-South)
8	3/30/93	7968, TR, B			
9	3/30/93	6107, BR, T			
10	3/30/93	6107, BR, B			
11	3/30/93	7968, TR, S			
12	3/30/93	6107, BR, S			
42	10/28/93	7188/7968, BC	Facing up, open		
43	10/28/93	7188/7968, BC	Facing down, open		
44	10/28/93	7188/7968, BC	Facing down, sheltered		
45	10/28/93	7188/7968, BC	Facing up, sheltered		
13	4/6/93	E	N8 (concrete)	115842, TR, T	With TOW instrumentation and corrosion coupons
14	4/6/93			115842, TR, B	
15	4/6/93			114764, BR, T	
16	4/6/93			114764, BR, B	
17	2/11/93	E	— (concrete)	144006, T	Empty cylinder stored separately at yard entrance
18	2/11/93			144006, B	
19	6/28/93	K	10 (concrete)	101379, TR, T	Heavily corroded cylinders, with corrosion coupons (no TOW instrumentation)
20	6/28/93			101379, TR, B	
21	3/30/93			17778, BR, T	
22	3/30/93			17778, BR, B	

Table 1 (continued)

Probe No.	Start Date	Yard	Row	Cylinder No., Probe Location	Comments
27	6/10/93	K	4 (concrete)	8726, TR, T	Lightly corroded cylinders, with corrosion coupons (no TOW instrumentation). Probes 31 and 24 inside skirts, along bottoms
28	6/10/93			8726, TR, B	
29	6/10/93			7243, BR, T	
30	6/10/93			7243, BR, B	
31	6/10/93			7243, BR, S	
24	6/28/93			8726, TR, S	
46	10/28/93			8726/6138, BC	Facing up, open
47	10/28/93			8726/6138, BC	Facing down, open
48	10/28/93			8726/6138, BC	Facing down, sheltered
49	10/28/93			8726/6138, BC	Facing up, sheltered
32	5/10/93	K	3 (concrete)	8177, TR, S	Heavily corroded cylinders (no coupons or TOW instrumentation). Probes 32 and 33 inside skirt bottoms, 5 under top of skirt, 23 and 6 above top of skirt
33	5/10/93			8370, BR, S	
5	7/7/93			8177, TR, S	
23	7/7/93			8177, TR, S	
6	7/7/93			8370, BR, S	
25	5/10/93	K	14 (gravel)	102193, BR, T	Lightly corroded cylinder (no corrosion coupons or TOW instrumentation)
26	5/10/93			102198, BR, B	
34	5/25/93	K	Coupon rack	—	Facing up, open
35	5/25/93			—	Facing down, sheltered
36	10/28/93			—	Facing up, sheltered
37	10/28/93			—	Facing up, open
38	10/28/93			—	Facing down, open
39	10/28/93			—	Facing down, open
40	10/28/93			—	Facing up, sheltered
41	10/28/93			—	Facing down, sheltered
54	12/13/93	K-1006 Loading Dock Area		—	Facing up, open
55	12/16/93			—	Facing down, open
56	1/5/94			—	Facing up, open, 45° slope

(TR – Top Row, BR – Bottom Row, BC – Between Cylinders, S – Skirt)

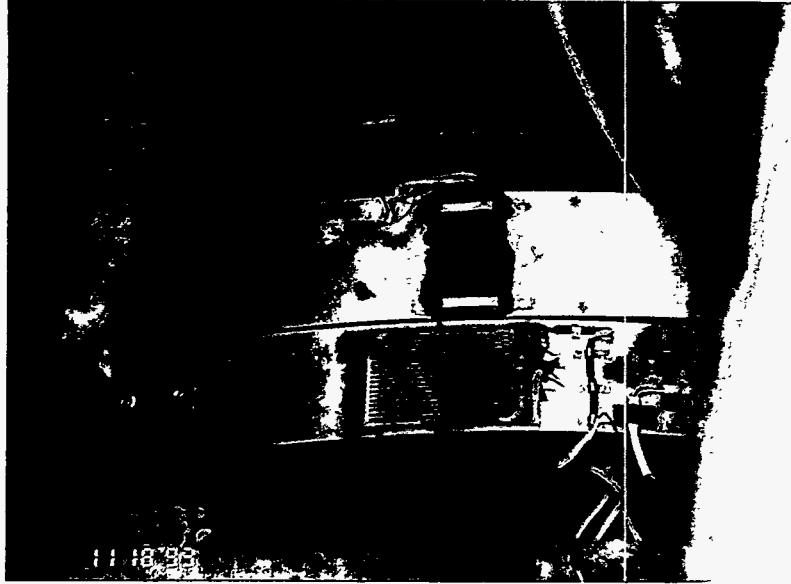


Fig. 3. Cylinder instrumented with time-of-wetness sensors; thermocouples and corrosion probes on stainless steel bands and one-sided corrosion coupons attached to cylinder surfaces with magnets.

3. RESULTS

A major objective of the program was to identify any differences in corrosivity as a function of cylinder location and stacking position. The three primary cylinder locations, representing varying water drainage and storage conditions, were chosen with this in mind. There are three main sources of data: TOW, corrosion probes, and corrosion coupons, and the results are presented separately below. Sensor/coupon locations are identified by stacking position and location on the cylinder. For example, TR, T refers to a position on top of a top-row cylinder, and BR, T refers to the top of a bottom row cylinder, etc.

Time-of-wetness

Table 2 shows an example of a typical TOW datalogger printout. Top-facing TOW sensors are the first to respond to the start of rain, quickly developing a near-full-scale signal response, and the relative humidity correspondingly increases to 100%. Although not seen in Table 2, the bottom-mounted TOW sensors also eventually show full-scale responses over periods of prolonged rain. This delay typically leads to lower measured TOW on bottom surfaces, as discussed below. Note also the variations in cylinder surface temperatures depending on location. Top surfaces heat up more in the daytime and show larger fluctuations over a 24-hour period. This is more apparent in the warmer months, and an example is discussed below.

TOW data and total monthly rainfall (average from rain gauges in E- and K-yards) over the length of the program (through July 1994) are summarized in Table 3. The TOWs are presented as the fraction of time the sensor was 'wet'. Since there are no standards, the onset of wetting was arbitrarily defined as an output of 200 mv. (The sensors have a full scale reading of 2500 mv.) Two main observations can be made from Table 3:

1. Sensors on top of cylinders tend to stay wetter than sensors mounted on cylinder bottoms, irrespective of yard or stacking position. Significant wetness on cylinder bottoms is observed mainly during months of the heaviest rainfall (March 1993, January through March 1994) although there are months when the extent of BR, B wetting does not correlate with the amount of rain (February 1993, December 1993, April 1994, June 1994).
2. In general, no significant difference in wetness times was observed between the well-drained concrete surface in E yard and the poorly drained broken concrete (K-South) area in K-yard. One may expect BR, B regions at K-South to stay wetter than in other areas because of poor drainage. However, as seen in Fig. 4, this is clearly not the case, and, in fact, the reverse may be true. In addition, Fig. 4(a) shows that cylinder tops in the gravel area at K-North appear to stay consistently drier than the other locations.

A detailed examination of the TOW results provides some clues to explain these observations. Figure 5 shows responses from TR, T and BR, B TOW sensors along with rainfall data collected during two time periods in April 1994 at the K-South location. The results are typical of all three locations. As can be seen, there are several instances when the TR, T sensor triggered a positive response over time periods with no rainfall. These include the early morning hours of April 2, 4, 5, 10, and 12. In each of these instances, the remaining three sensors at the installation did not trigger. The positive responses are apparently caused by dew formation on the sky-facing top surfaces during the early morning hours. Similar observations have been commonly reported in the

Table 2. Typical time-of-wetness (TOW) data, gathered over an 8-hour period in E-yard

Date	Time	TC1 ^a (°F)	TC2 ^b (°F)	TC3 ^c (°F)	TC4 ^d (°F)	Rain (")	TOW1 (mv)	TOW2 (mv)	TOW3 (mv)	TOW4 (mv)	RH1 ^e (%)	AT1 (°F)	RH2 ^f (%)	AT2 (°F)
2/20/93	20:00	40.6	37.9	39.5	37.4	0.00	0	370	0	90	77	38.7	58	38.2
2/20/93	20:30	39.2	39.0	39.5	37.9	0.00	40	460	0	100	82	38.7	60	38.2
2/20/93	21:00	39.2	38.1	38.6	37.1	0.00	150	510	0	130	83	38.2	62	38.2
2/20/93	21:30	39.2	38.6	38.6	37.1	0.00	0	520	0	130	84	38.2	63	38.2
2/20/93	22:00	38.1	38.6	39.2	38.1	0.00	120	530	260	150	85	38.2	64	38.2
2/20/93	22:30	38.1	37.6	38.1	37.6	0.01	2260	770	2180	220	98	37.7	73	38.2
2/20/93	23:00	39.2	38.1	38.1	37.6	0.02	2400	1100	2400	320	100	37.7	87	38.7
2/20/93	23:30	38.1	39.2	39.2	38.6	0.00	2420	1140	2420	340	100	37.7	92	38.7
2/21/93	00:00	38.1	38.1	38.1	37.6	0.00	2420	1140	2420	340	100	37.2	95	38.7
2/21/93	00:30	38.1	38.1	38.1	38.1	0.00	2420	1120	2430	340	100	37.2	96	38.7
2/21/93	01:00	38.1	38.1	38.1	38.1	0.00	2420	1100	2430	340	100	37.2	97	38.7
2/21/93	01:30	38.1	38.1	38.1	38.1	0.00	2420	1080	2430	330	100	37.2	98	38.7
2/21/93	02:00	38.6	38.1	38.6	38.1	0.00	2430	1050	2440	320	100	37.2	98	38.7
2/21/93	02:30	38.6	38.1	38.6	38.1	0.01	2440	1030	2450	310	100	37.2	98	38.7
2/21/93	03:00	38.1	38.1	38.1	38.1	0.01	2460	1010	2460	300	100	37.2	99	38.7
2/21/93	03:30	38.0	38.1	38.6	38.1	0.05	2450	1000	2450	300	100	37.2	99	38.7

^aTC1 and TOW1—TR, T thermocouple and TOW sensor.

^bTC2 and TOW2—TR, B thermocouple and TOW sensor.

^cTC3 and TOW3—BR, T thermocouple and TOW sensor.

^dTC4 and TOW4—BR, B thermocouple and TOW sensor.

^eRH1, AT1—relative humidity and ambient temperature from weatherhead 1.

^fRH2, AT2—relative humidity and ambient temperature from weatherhead 2.

Table 3. Monthly data from the three time-of-wetness sensor sets

	E-Yard (Concrete) (% Time Wet)*				K-Yard North (Gravel) (% Time Wet)				K-Yard South (Concrete) (% Time Wet)				Total Rain (")
	TR, T	TR, B	BR, T	BR, B	TR, T	TR, B	BR, T	BR, B	TR, T	TR, B	BR, T	BR, B	
Feb. 93	35.9	46.7	57.7	32.1	31.2	8.2	32.7	13.3	41.7	6.2	37.5	16.8	4.32
Mar. 93	50.9	62.8	55.3	45.5	41.0	13.2	38.3	37.1	57.9	10.2	52.8	28.4	7.0
Apr. 93	34.3	12.7	20.6	11.5	17.8	0	14.0	0	28.1	0	16.6	0	3.39
May 93	35.6	13.0	25.4	3.7	26.3	2.0	18.9	3.0	45.0	0	22.7	0	2.76
Jun. 93	—	0	17.1	0	10.9	0	10.9	0	—	0	16.4	0	1.5
Jul. 93	10.8	1.4	9.6	0.1	5.0	0	5.2	0	13.5	0	11.2	1.3	2.15
Aug. 93	23.4	0.1	20.1	0.1	9.7	0	9.0	0.1	25.8	0	16.4	0	3.48
Sep. 93	37.7	0.8	28.6	3.1	28.5	0	16.9	6.6	42.6	0	27.7	4.8	4.03
Oct. 93	46.2	8.1	34.2	17.1	37.8	3.3	22.9	20.35	48.1	3.0	35.8	16.5	1.92
Nov. 93	—	—	—	—	—	—	—	—	—	—	—	—	3.25
Dec. 93	40.2	5.9	28.3	6.7	27.4	3.4	28.5	6.9	33.9	3.3	37	4.2	6.68
Jan. 94	37.1	38.2	15.6	38.8	31.8	30.0	34.7	27.6	36.9	33.1	45.9	20.8	6.35
Feb. 94	34.5	21.1	17.8	38.8	28.7	26.0	29.7	38.2	34.0	23.8	32.0	27.6	9.6
Mar. 94	35.0	5.0	13.0	11.0	33.0	5.0	28.0	17.0	30.0	21.0	29.0	25.0	10.25
Apr. 94	25.0	1.0	5.0	13.0	20.0	1.0	14.0	16.0	24.0	1.0	14.0	12.0	8.82
May 94	27.0	0	13.0	0	16.0	0	10.0	3.0	26.0	0	15.0	0	2.77
Jun. 94	27.0	0	24.0	0	17.0	0	14.0	2.0	28.0	0	32.0	4.0	7.43
Jul. 94	36.0	0	27.0	6.0	24.0	0	19.0	3.0	34.0	0	35.0	9.0	5.93

*Wetness is shown as the percentage of time that sensor responses were above 200 mv. "—" indicates a lack of data due to equipment malfunction.

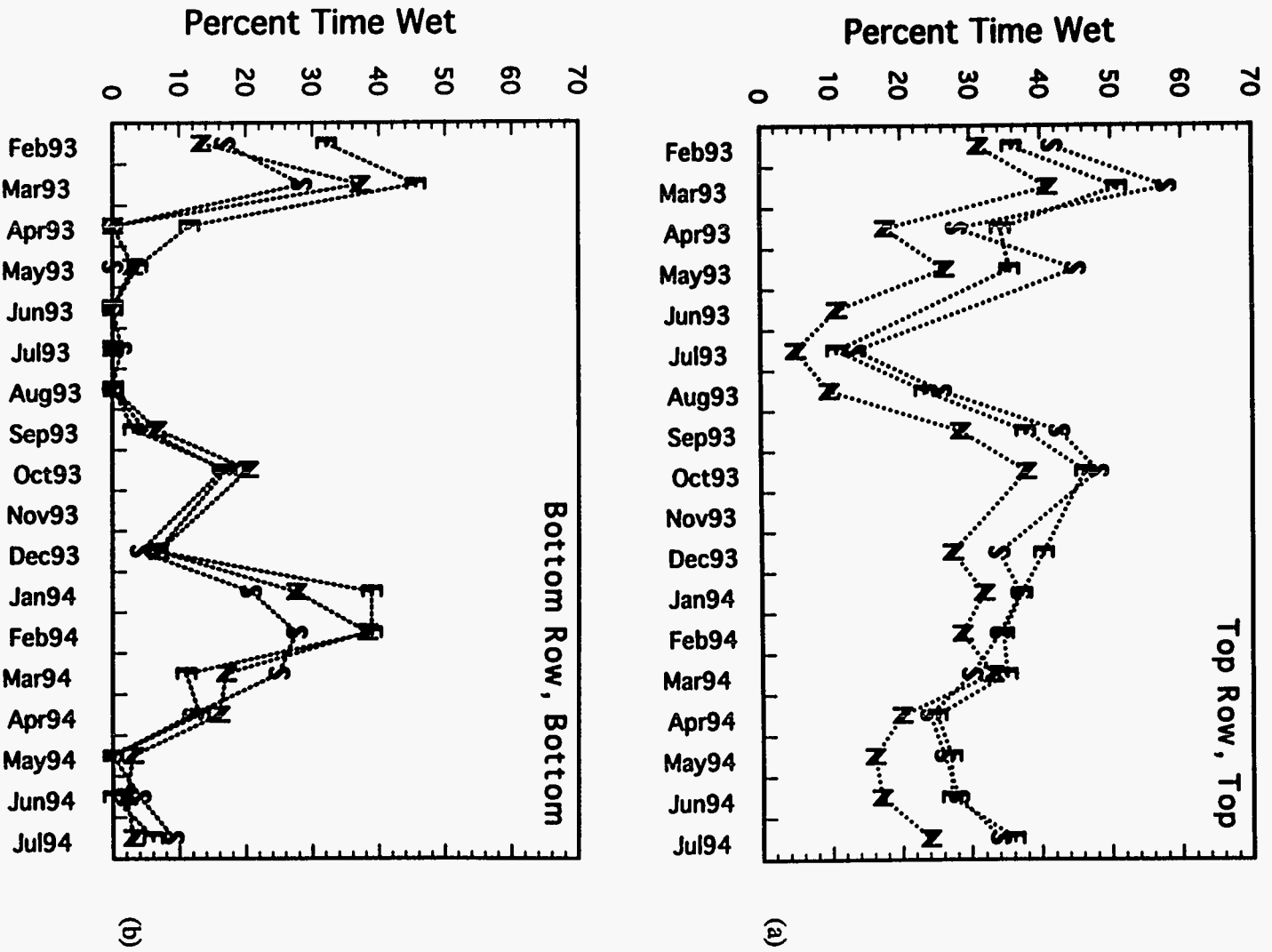


Fig. 4. Percent wetness measured in (a) top row, top positions and (b) bottom row, bottom positions. E = E-yard, N = K-yard north (gravel) and S = K-yard south (concrete).

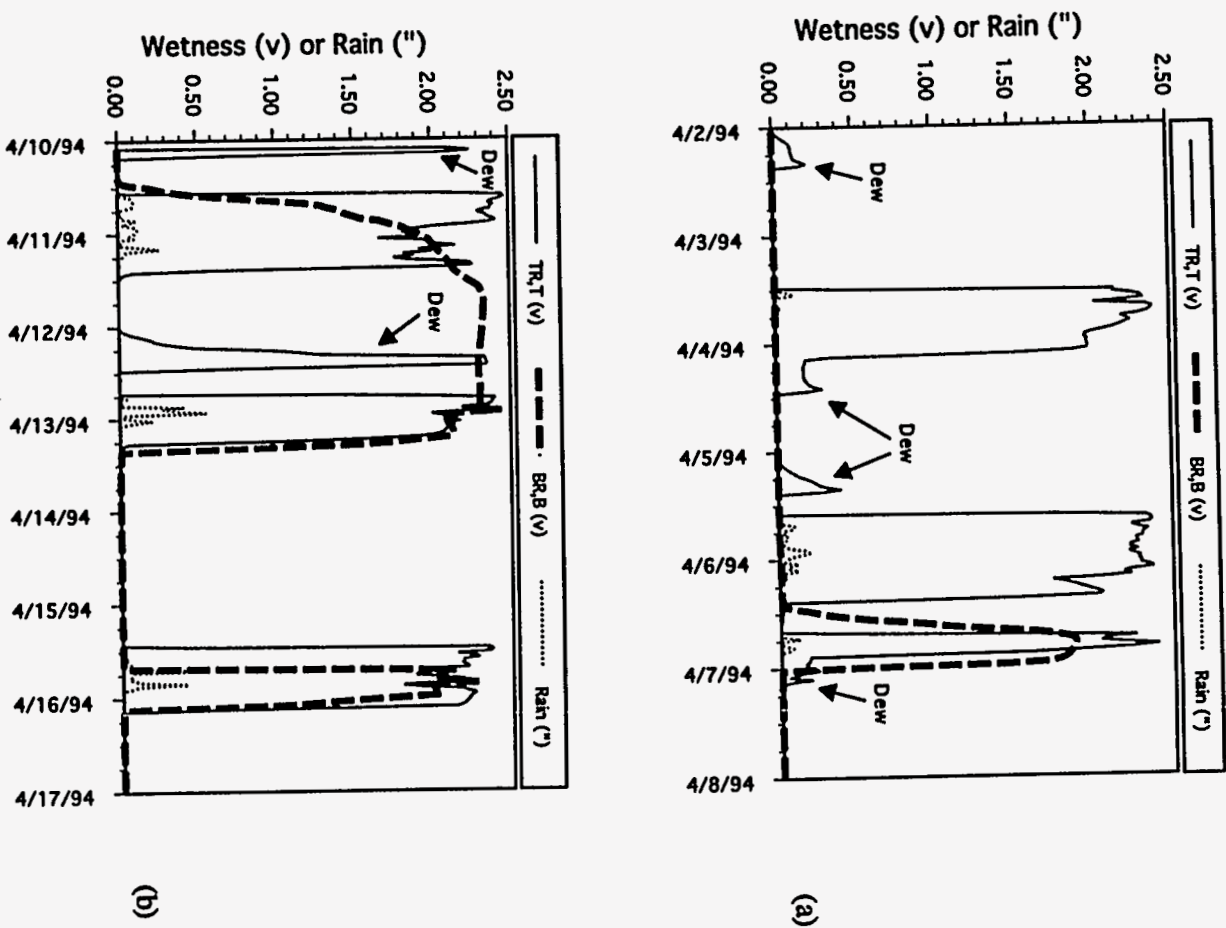


Fig. 5. (a) and (b) Wetness data from top row, top and bottom row, bottom sensors along with rainfall data collected during two time periods in April 1994 at the K-yard south location.

past,^{9,10,17,18} as has the fact that condensation can be the major contributor to total wetness times^{9,17} and often triggers a lower sensor response than rain,¹⁹ as observed here. The top surfaces undergo greater cooling due to radiative heat loss than bottom-facing surfaces, and surface temperatures are more likely to go below the dew point, leading to condensation. This is supported by thermocouple data from the cylinder surfaces. Data from the same time period as Fig. 5(a) from TR, T and BR, B surfaces at K-South are shown in Fig. 6. It is clear that the TR, T surface undergoes much greater temperature swings during a 24-hour period than the BR, B surface, which stays fairly close to ambient temperatures. The large fluctuations are due to a combination of radiative heating and cooling, the effects of which are magnified by an empty head space in the UF₆ cylinders, whereas temperature variations of bottom surfaces are moderated by the large heat mass of UF₆ in contact with these surfaces. During 1 day, both the highest and lowest temperatures are measured on cylinder tops, which evidently cool down below the dewpoint at night, causing condensation. Note that on April 3, there was no apparent dew formation [Fig. 5 (a)]. This condition can be related to significantly less cooling of the cylinder surface (Fig. 6), probably due to cloud cover before the rain later in the day [Fig. 5 (a)].

Figure 5 reflects the conclusion from Table 3 that cylinder tops stay significantly wetter than cylinder bottoms, but also provides further details. The rain events on April 4 and April 6 were insufficient to trigger the BR, B sensor: the sensor triggered only over the next rain period on April 7. It triggered again on the next rain on April 11, but this time the sensor stayed “on” for 3 days even though no rainfall was measured and the TR, T sensor switched off. These results suggest that cylinder bottoms stay dry even during rain periods, until a critical frequency and/or amount of rain

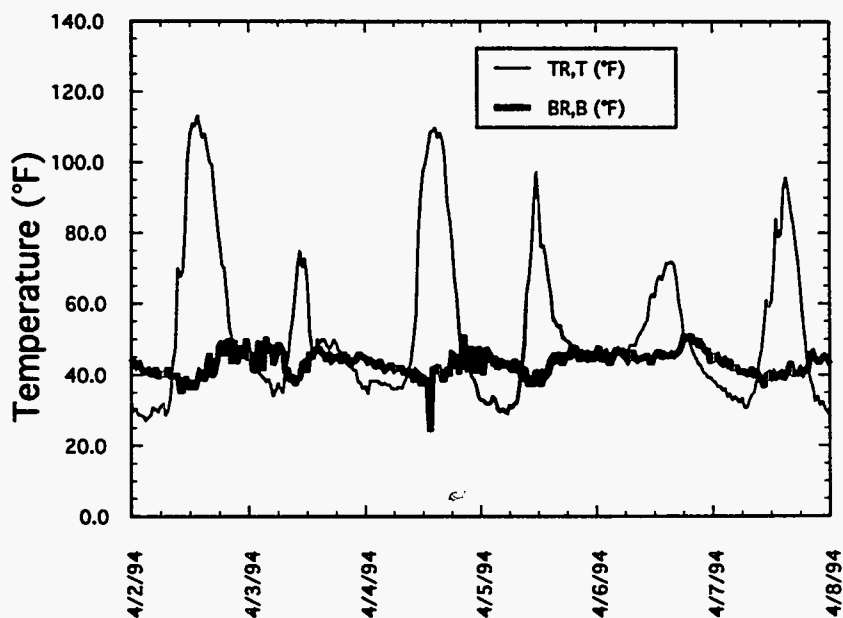


Fig. 6. Surface temperature data from TR,T and BR,B surfaces at K-yard south for the same time as Fig. 5(a) showing much greater temperature fluctuations on TR,T surfaces due to radiative heating and cooling.

is exceeded. Once the bottoms are wet, they apparently stay wet longer than top surfaces, also perhaps related to the frequency of rain/dampness/cloudiness during the period of drying.

This view is supported by the data in Figs. 7 (a) and (b), which show rainfall data as well as periods when TR, T and BR, B TOW sensors were "on" during December 1993 and January 1994. (Some of the precipitation occurred in the form of ice or snow. However, sunshine and/or daytime temperatures typically melted the solid precipitation on contact or within a few hours. There was only one instance, toward the end of January, when solid precipitation was present for a period greater than 24 hours.) The time intervals shown, 27 days in Fig. 7(a) and 34 days in Fig. 7(b), experienced roughly equal amounts of total rain. In the period shown in Fig. 7(a), the BR, B sensor was triggered only over two time periods representing 6.8% of the time interval, compared to a 39.6% "on" time for the TR, T sensor. In contrast, for the period shown in Fig. 7(b), both TR, T and BR, B sensors stayed "on" for 38.3% of the time. It may be noted that the response of the TR, T sensor was very similar over the two time periods. The difference between Figs. 7(a) and 7(b) is that, in the first case, rain events were relatively heavy but few, typically occurring every 5 days. During the second time period, rain was less heavy but occurred more frequently. Note that, toward the end of January with several rain events over the last few days, the BR, B sensor stayed "on" for more than 1 week. This observation is similar to one made earlier with respect to Fig. 5(b). Note also that in both Figs. 7(a) and 7(b), the initial triggering of the BR, B sensor was always significantly after that of the TR, T sensor. These data support the conclusion that cylinder bottoms stay drier than cylinder tops because a significant amount of frequent precipitation is needed for the wetness to reach and cover these areas. The critical value of this precipitation is unknown but could perhaps be estimated from detailed analysis of a few months of data. This analysis has not yet been attempted.

One relationship which could not be established conclusively was that between relative humidity and TOW. The relative humidity sensors typically broke down after 2-3 months, and practical considerations prevented immediate replacement of the sensors. Figure 8 presents summaries of relative humidity readings taken at the same time as TOW responses from the TR, T sensor in E-yard for the months of February 1993 (just after installation) and April 1993. In February 1993, almost all the nearly full-scale TOW responses corresponded to relative humidities greater than 50%, with a large fraction occurring at relative humidities of over 90% (mostly at 100%). In contrast, in the month of April 1993, the high TOW responses are distributed over the entire range of relative humidities, indicating that the humidity sensors were not responding consistently. The highest reading recorded was 92%, even during periods of rain. By the following month, maximum sensor response had dropped further, signifying sensor failure.

While the sensors were working, a fairly good correlation was shown between relative humidity and TOW readings. It appeared that the TOW sensors showed a positive reading only when relative humidity levels were over 50% and had readings over 200 mv (the "on" threshold) only at relative humidity readings greater than 60-70%. This agrees well with observations in the literature.^{5,9,10,15,17,19} Data were insufficient to do a rigorous correlation analysis over different seasonal periods. In addition, the relative humidity sensors were in the weatherheads, located a few feet away from the TOW sensors. Thus, local variations in relative humidity due to cylinder surface temperatures or ground conditions could not be determined. These variations could be significant⁴ and could lead to local differences in wetness and corrosion. Current plans call for installing relative humidity sensors next to the TOW sensors.

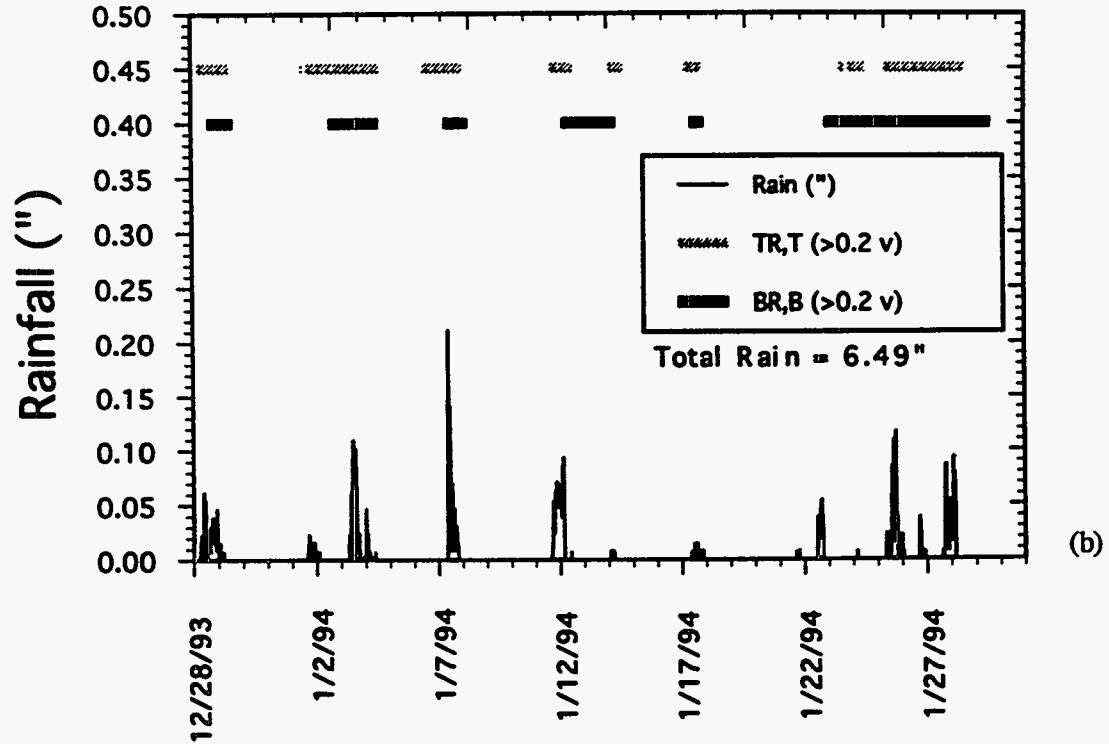
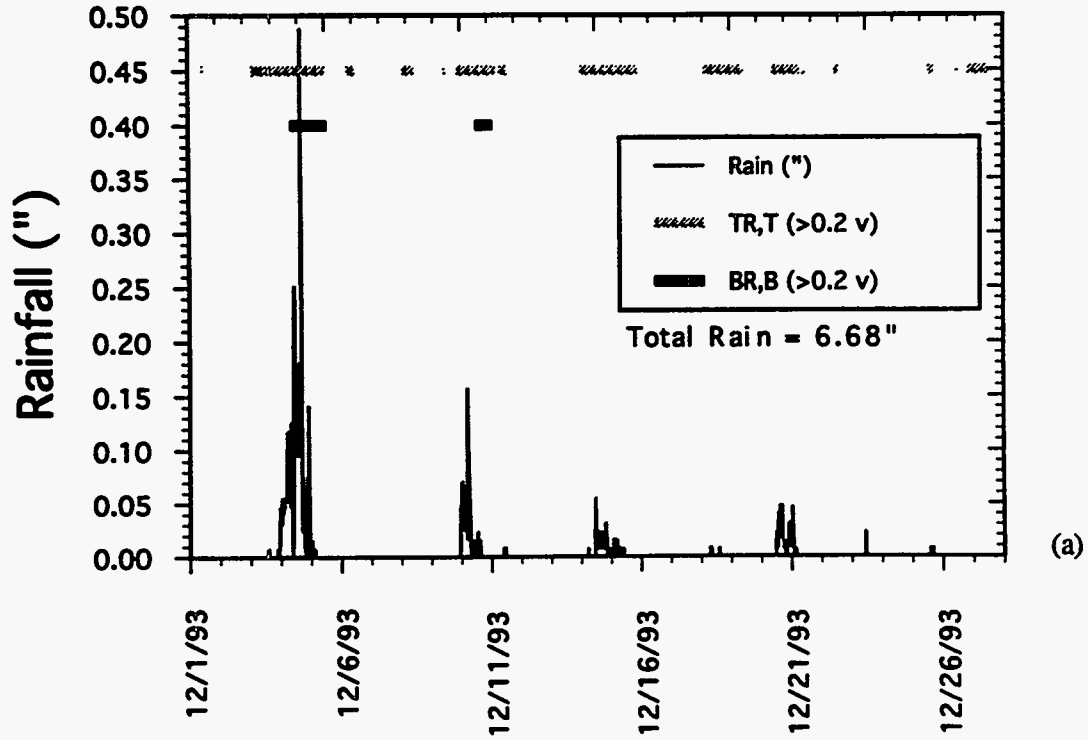


Fig. 7. (a) and (b) Rainfall data and periods when TR,T and BR, B time-of-wetness sensors were "on" during December 1993 and January 1994 at the E-yard location.

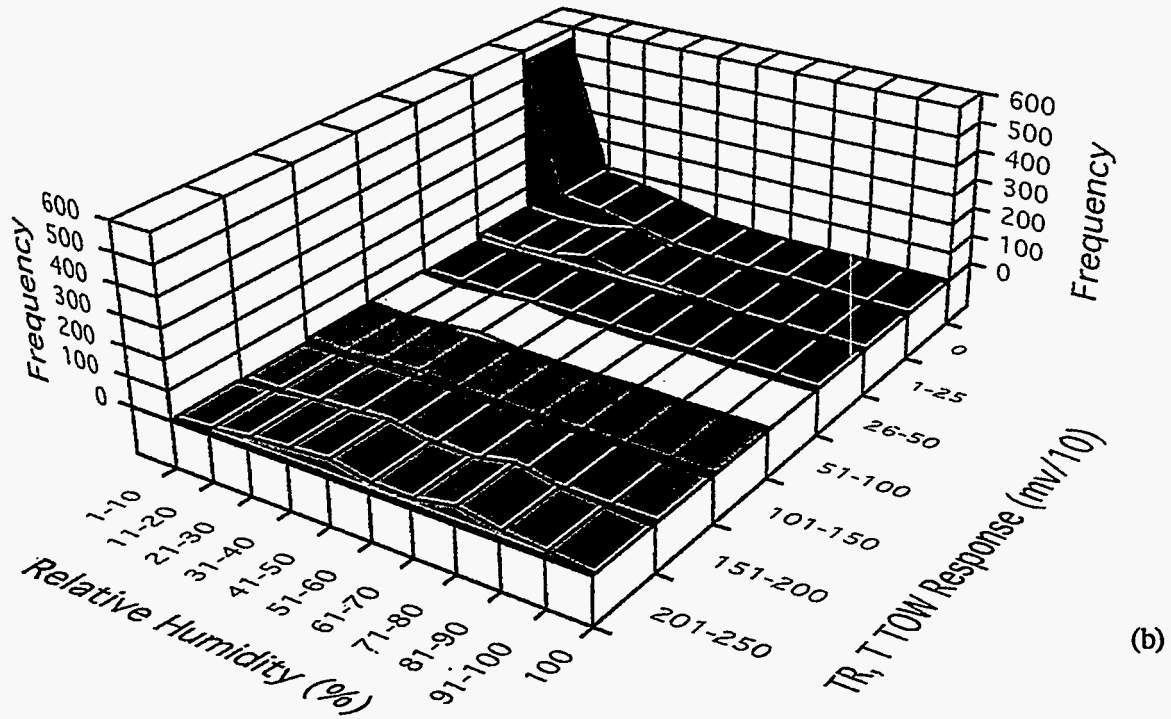
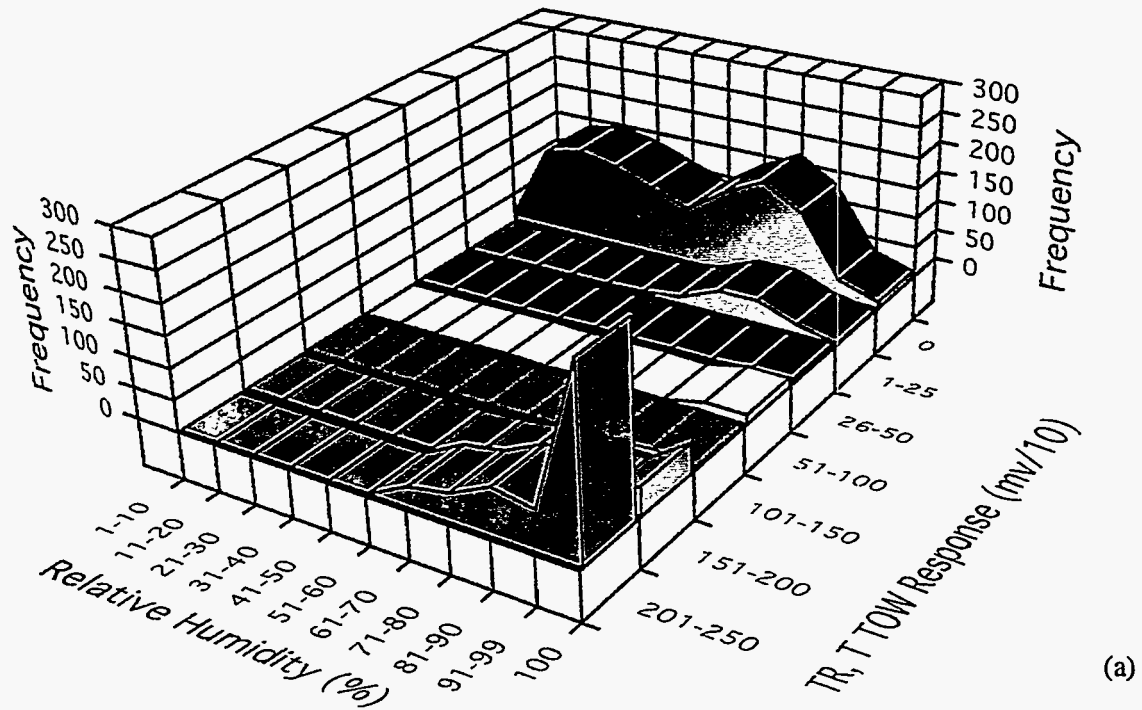


Fig. 8. Relative humidity and corresponding time-of-wetness sensor responses from E-yard for the months of (a) February 1993 and (b) April 1993.

Corrosion probes

The corrosion probes were installed mainly between late March and early July 1993. Results from the various locations have generally been similar. No differences have been observed between K-yard or E-yard, or between locations within a yard. All differences in data appear to be directly related to the orientation of the probes. Figure 9 shows typical data, from the K-North location. Corrosion rates are measured as the slopes of the metal loss vs time plots. Several trends may be noted:

1. Probes exhibit an incubation period before the probe dial readings begin to increase (i.e., before measurable corrosion occurs). The incubation period is significantly longer on probes attached to bottom surfaces of cylinders.
2. Probes show similar trends depending on whether they are mounted on top or bottom surfaces, irrespective of whether the cylinder is in a top or a bottom row.
3. Significantly higher corrosion rates (measured after incubation) are observed from probes on cylinder tops than from probes on cylinder bottoms. However, these corrosion rates appear to moderate in some cases at later stages (e.g., Probe 3 in Fig. 9).

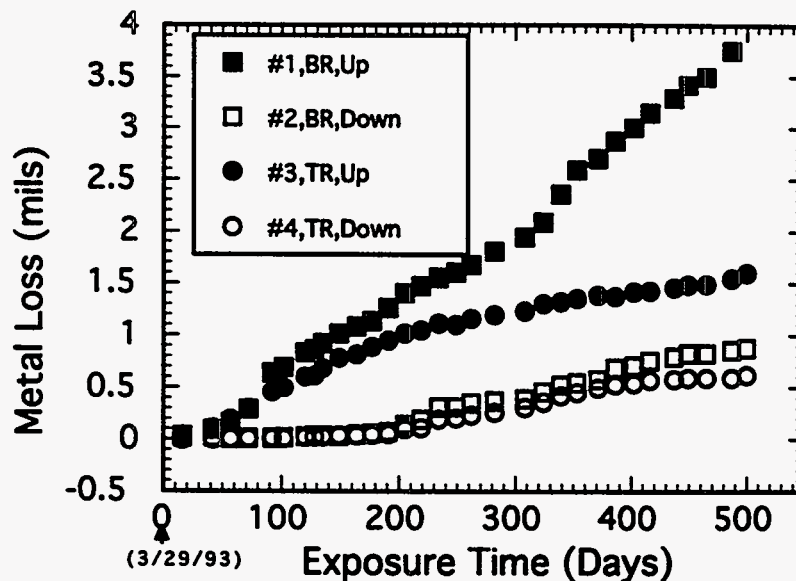


Fig. 9. Typical corrosion probe data, for Probes 1-4 mounted on cylinders at the K-yard north location.

Figure 10(a) shows data from a set of probes attached to the corrosion coupon rack in K-yard. These probes were attached in orientations shown in Fig. 10(b), meant to replicate probes on cylinders. The trends seen in Fig. 10(a) are very similar to those seen in Fig. 9. Top-facing open probes (34 and 37) have shorter incubations and corrode faster, at least initially. The moderation in corrosion rates (change in slope) typically occurred after about 200 days of exposure for most top-facing probes (see also Fig. 9). Note that sets of probes were installed in late May and late October, yet show similar trends. This suggests that any seasonal effects on corrosion are minimal, although a careful analysis shows that they cannot be discounted. Metal loss vs time data for all the probes were examined, and 32 probes were identified, which showed a decrease in the slope (corrosion rate) in the post-incubation region. For example, such decreases in slope can be seen in Fig. 9 as occurring for Probe 3 after about 210 days and Probe 4 after 400 days. A clearer example can be seen in Fig. 10(a) for Probe 34 after 150 days. A tabulation of all the data showed that in 16 of the 32 cases, the decrease in slope was initiated in the months of November through January, suggesting a wintertime slowdown in corrosion rates. However, 14 of these 16 "slowdowns" occurred starting 150-230 days from initial exposure and 15 of the 16 probes were top-facing open probes, suggesting that the "slowdown" is more related to the time-dependent buildup of certain types of corrosion products. This issue is currently unresolved. It may also be noted that many probes showed an increase in corrosion rate after some period of "slowdown," typically from 60 to 90 days [see Fig. 10(a)].

Although the general behavior of top- and bottom-facing probes as two separate groups is similar, there are differences in individual probe behavior which are unexplained. An example is Probe 1 in Fig. 9. The lack of a transition to a lower corrosion rate is unusual and cannot be explained at present. Similarly, in Fig. 10(a), top-facing open Probes 34 and 37 appear to diverge significantly in behavior after showing similar responses for the first 150 days of exposure. In this set of probes, only Probe 34 among the "open" installations appears to show an interim transition to a lower corrosion rate. Further, the subsequent increase in corrosion rate in Probe 34 after 320 days is also unexplained. Some of these discrepancies must surely be related to seasonal changes and chemistry and morphology of the corrosion products developed on the probes. Recently, three of the probes (including Probe 1 in Fig. 9) reached the end of useful data collection life and "topped out," having undergone 4 mils of metal loss. These probes will be destructively analyzed, and it is hoped that corrosion product analysis and continuing data collection will help resolve some of the questions regarding probe behavior.

Figure 11 summarizes the corrosion probe data from several locations, including the three primary locations, the coupon rack and several other installations in K-yard. The data are presented as corrosion rates calculated from plots as in Figs. 8 and 9(a). As seen in these figures, the plots can often be divided into several linear segments having different slopes (i.e., different corrosion rates). Corrosion rates after "150 days" represent corrosion rates existing after 150 days exposure, which typically corresponds to post-incubation for top-facing probes but often still within incubation for down-facing probes. Data for ">300 days" for all probes represent the trend being observed in the last 100 days of data gathering. Total exposure periods range from approximately 300 to 500 days. Figure 11 shows that in most cases, corrosion rates of top-facing probes decreased significantly after initial incubation and a period of relatively high corrosion rate. The ">300 days" corrosion rates are often similar to those measured from down-facing probes, which typically show minimal corrosion for relatively long time periods before exhibiting a slight upward trend in corrosion rates. The data summarized in Fig. 11 show no obvious effects of poor or good drainage or of yard-to-yard differences.

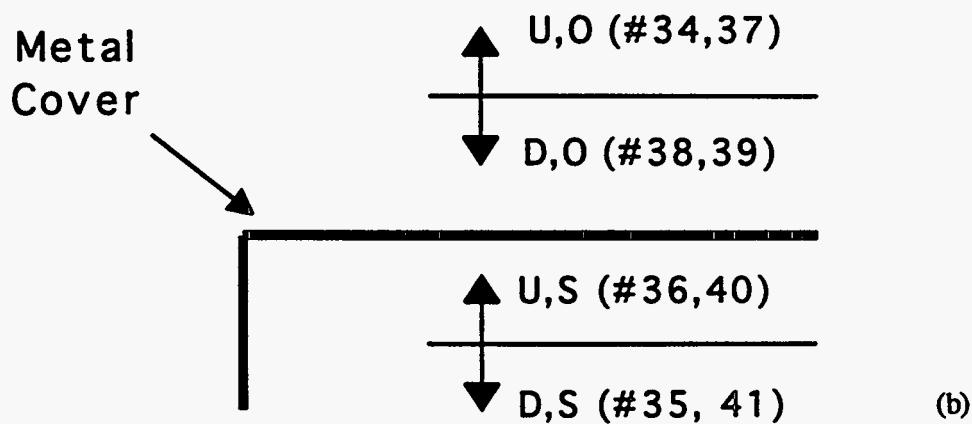
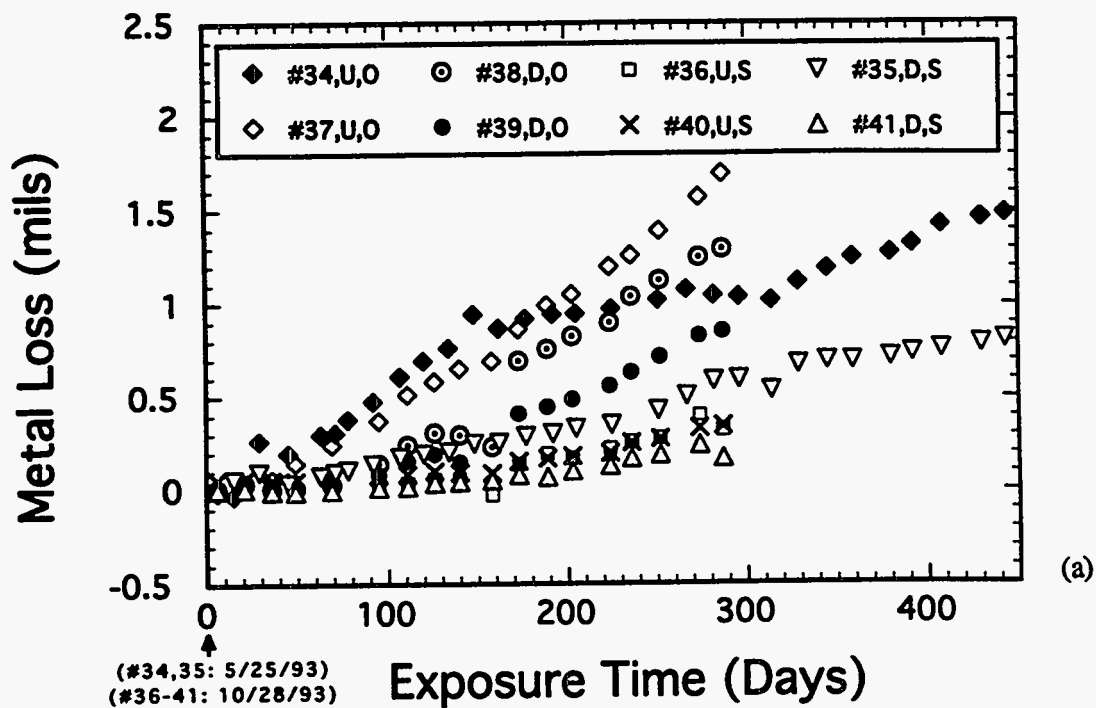


Fig. 10. (a) Corrosion probe data from probes installed in various orientations on the coupon rack in K-yard. (b) Schematic showing the orientations of probes. The arrows point in the direction the probe is facing. (U, O = up; open; D, O = down, open; U, S = up, sheltered; D, S = down, sheltered.)

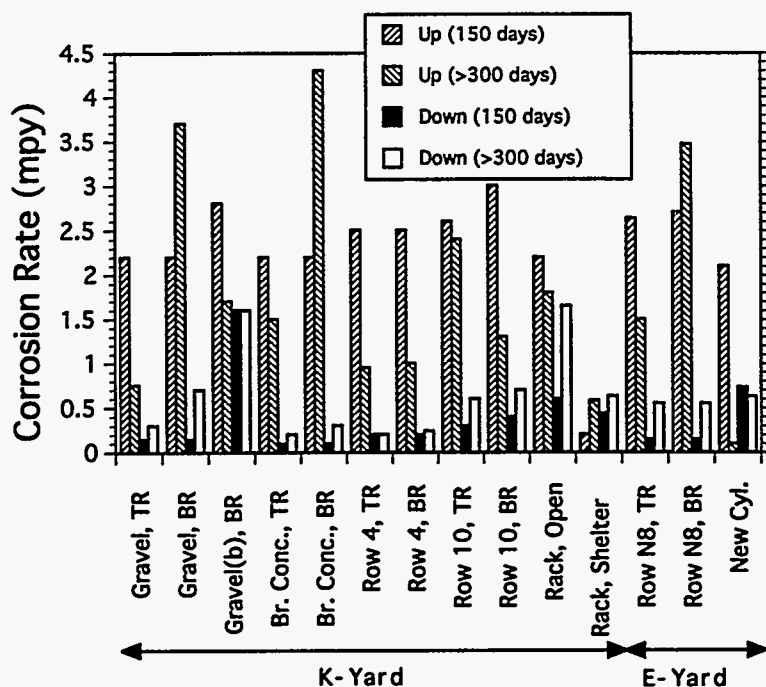
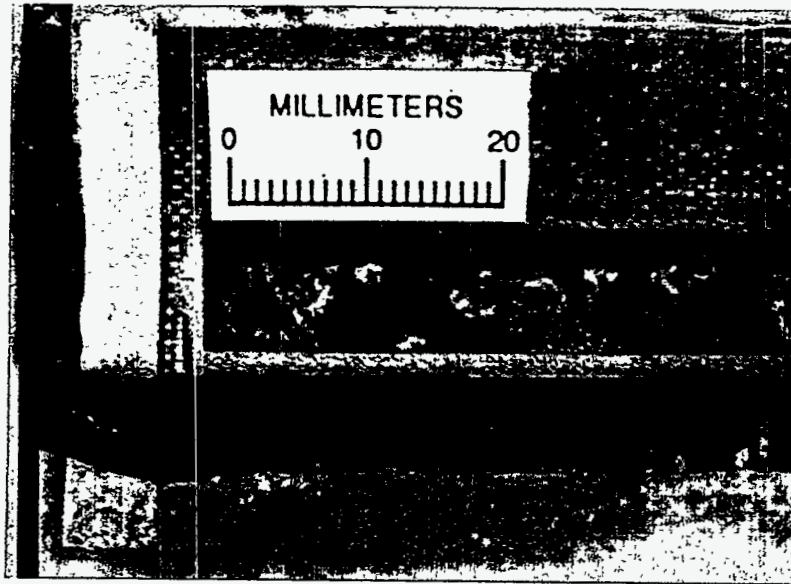


Fig. 11. Corrosion rates calculated from data from corrosion probes.

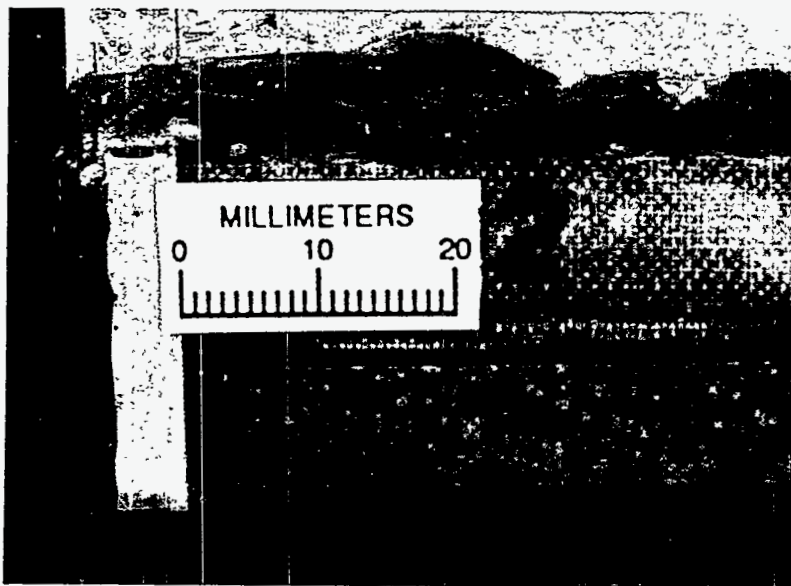
The long incubation periods and low corrosion rates associated with the down-facing probes (which include bottom-mounted probes on cylinders) are also seen in top-facing probes, which are sheltered [Fig. 10(a), Probes 36 and 40]. (This arrangement is not duplicated on the UF_6 cylinder surfaces, since all top-facing cylinder probes are open to the sky.) Top-facing sheltered probes evidence less corrosion than down-facing open probes (Probes 38 and 39). These results imply that surfaces protected from wetting undergo less corrosion, at least to the point that the onset of corrosion is delayed significantly. As a further check, three sets of probes were distributed in spaces between top-row cylinders in K-yard in the orientation shown in Fig. 10(b). The results are very similar to those observed in Fig. 10(a).

Figure 12 shows photographs of part of the active element of Probes 1 (BR,T) and 2 (BR, B) after 158 days exposure. The top-facing probe was completely covered with a flaky, orange rust layer, whereas the bottom-facing probe still had large uncorroded areas visible. This clearly shows that the extended incubation and negligible initial corrosion rates observed in bottom-facing probes can be related to a delay in the start of the corrosion process. Figure 13 shows Probes 1 and 2 after 500 days exposure, when the corrosion rate on Probe 2 had increased significantly. The higher corrosion rate can be related to the appearance of corrosion product on the probe.

To relate probe response more closely to changes in its appearance and weather, three probes were installed in the loading dock area of the laboratory building: one horizontal and facing up (Probe 54), the second horizontal and facing down (Probe 55) and the third facing up but sloping downward at an angle of 45° (Probe 56), to allow water to drain off. Probes 54 and 55 were installed within 3 days of each other in early December 1993, and Probe 56 was installed about 20



(a)



(b)

Fig. 12. Corroding elements of Probes 1 and 2 after 158 days of exposure. (a) Probe 1, K-yard north, bottom row, top. (b) Probe 2, K-yard north, bottom row, bottom.

Fig. 13. Corroding elements of Probes 1 and 2 after 500 days of exposure. (a) Probe 1, K-yard north, bottom row, bottom. (b) Probe 2, K-yard north, bottom row, top.



days later in early January 1994. The probes were monitored at least daily for the first few weeks of exposure. The data are summarized in Fig. 14. Again, the bottom facing probe (55) shows the longest incubation time, but shows a corrosion rate similar to the top facing Probe 54 once corrosion starts. Both Probes 54 and 55 undergo a significant drop in corrosion rates after about 120 days of exposure. Probe 56 does not show a well-defined incubation or any significant changes in slope over the data collection period. The corrosion product appears to be darker and thinner than on the other probes but has not been analyzed. In the final 30 to 50 days of data collection, the slopes in all three cases are fairly similar (though still higher for the top-facing Probe 54), indicating a narrowing of differences as reported above.

Visual inspections showed that Probe 54 quickly developed a rust layer on its surface (completely rust covered within 7 days) whereas Probe 55 had large rust-free areas even after 40 days of exposure. Probe 56 showed intermediate behavior while developing a thinner, darker, more adherent corrosion product. During rain events, Probes 54 and 56 were quickly wetted whereas Probe 55 stayed mostly dry, with occasional wetting from wicking action of water beads forming on the edges of the covering surface. Furthermore, Probe 54 stayed wet for significant periods (often on the order of 1 day) after rain ended, whereas Probe 56, inclined at 45°, dried off within a couple of hours. Figure 15 shows photographs of the two top facing probes following a rainfall event. The beads of water seen on the probes were typical of observation even after short periods of rain. The water drops overhanging the edge of Probe 54 occasionally wicked onto the surface of Probe 55 directly underneath, initiating corrosion.

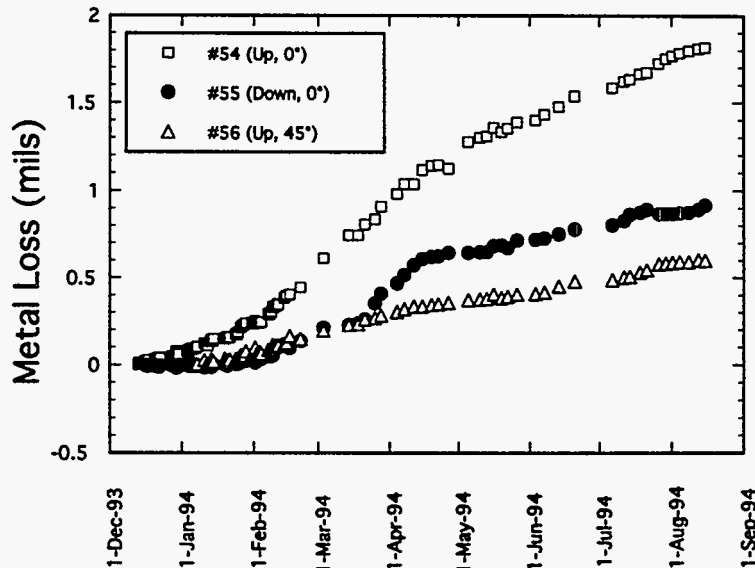
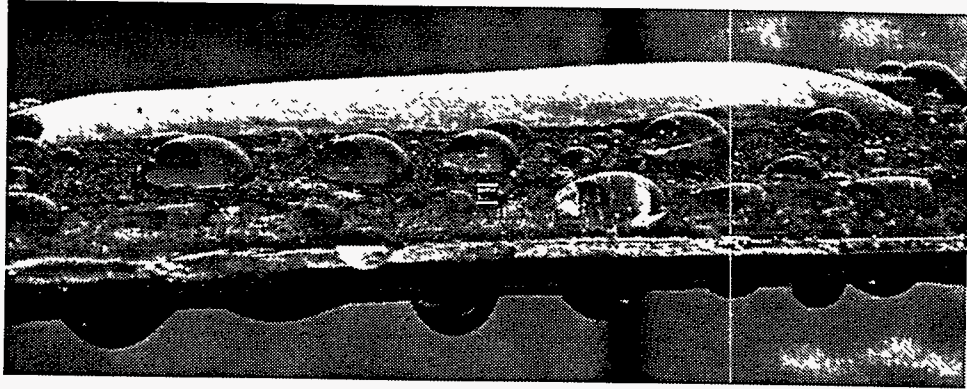
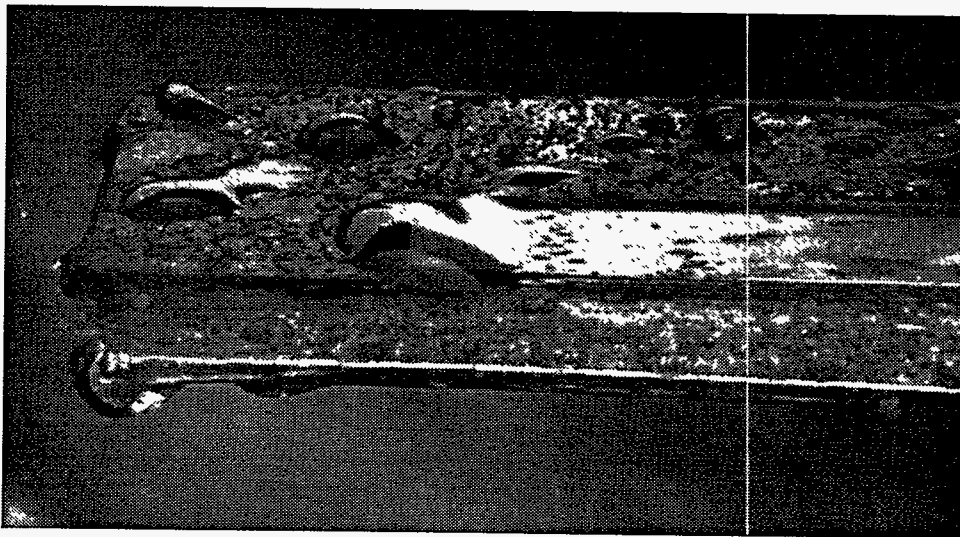


Fig. 14. Data from corrosion probes mounted outside the laboratory area.



(a)



(b)

Fig. 15. Photographs of (a) Probe 54 (mounted facing up horizontally) and (b) Probe 56 (mounted facing up inclined at 45°) after a period of rain. Probe 55, which is not visible, is mounted directly beneath Probe 54.

Figure 16 shows data from Probe 54 covering a few periods of precipitation. Corrosion is clearly associated with periods of wetness but appears to increase after the end of the rain, as the water bead evaporates. Such discrete jumps in metal loss were not seen in the other two probes, and this observation agrees with the model of atmospheric corrosion of iron's being dominated by corrosion during the drying stage of a moisture deposition/evaporation cycle.²⁰ Figure 16 also presents ambient temperature data showing that the corrosion process does not seem to be influenced by the temperature, at least in the range encountered.

Metal loss vs exposure time data for the remaining probes are included in Appendix A.

Corrosion coupons

Data from 1- and 2-year exposures of ASTM G50 coupons are shown in Fig. 17. Higher corrosion rates were observed in the first year of exposure, as is typically observed in atmospheric exposures. In the second year, the corrosion rates drop off to 0.5-0.7 mpy, which is what may be expected in the rural or semi-rural atmosphere around Oak Ridge. One interesting trend which may be developing in Fig. 17 is the higher corrosion rates measured in E-yard. Compared to K-yard, the rates are at least 50% higher in the first year and about 30% higher in the second year. It is unclear whether the differences will narrow over the next set of retrievals.

Figure 18 shows data from 1-year exposures of cylinder coupons. The corrosion rates measured from these single-sided coupons are significantly higher than those from the 2-sided ASTM G50 coupons. Part of the reason is undoubtedly due to the sheltering of bottom surfaces in the latter case.

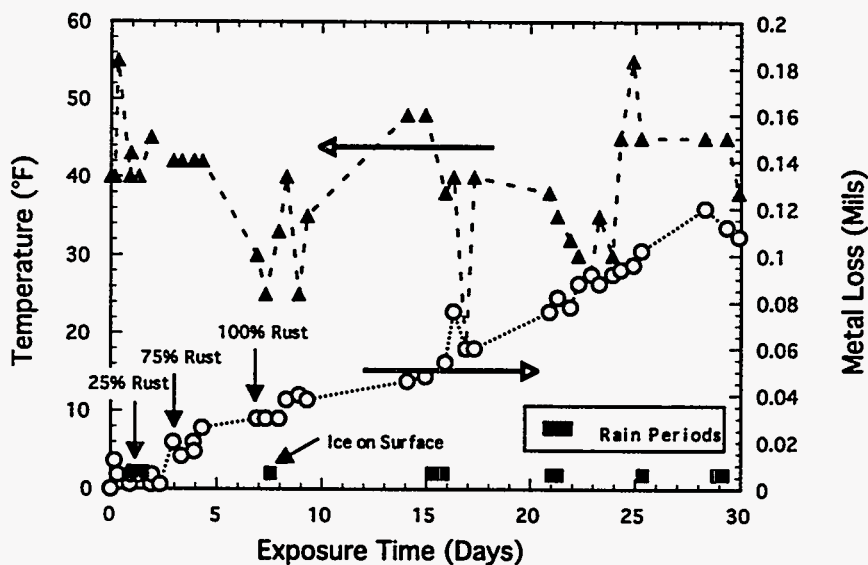


Fig. 16. Data from Probe 54 (mounted facing up horizontally) showing relationship between probe readings and periods of precipitation.

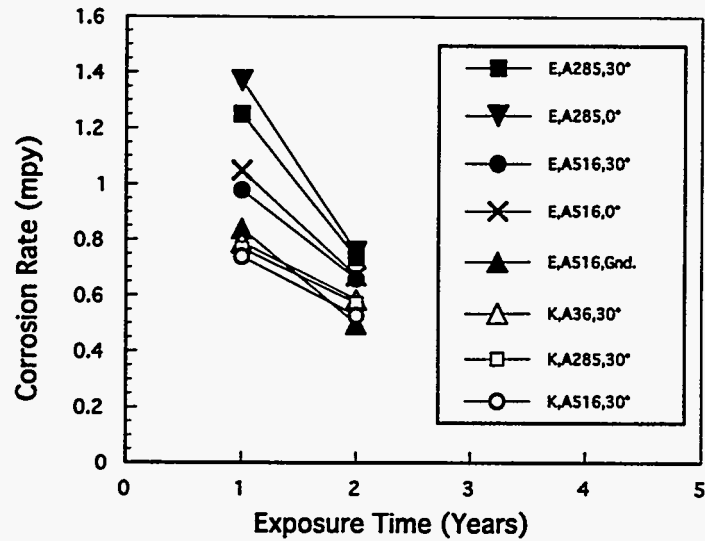


Fig. 17. Corrosion rates measured after 1- and 2-year exposure from ASTM G50 type coupons mounted on coupon racks in E-yard and K-yard. Only average values are shown; the scatter in each data set was typically less than 10%.

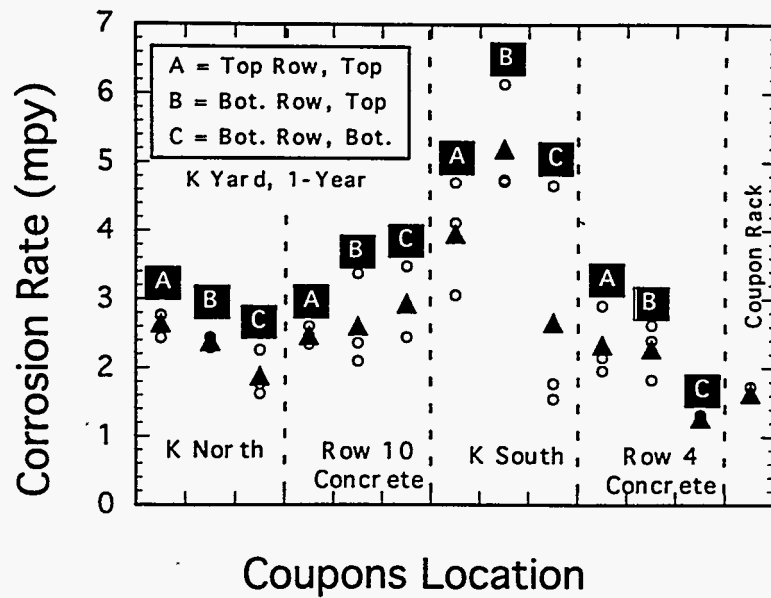


Fig. 18. Corrosion rates measured after 1-year exposure from coupons mounted on cylinders in K-yard. (○ = individual data points and ▲ = average values.)

There may also have been contributions from undercutting around the taped edges of the cylinder coupons. This was clear in some of the coupons in which the tape had delaminated in places and may also contribute to the larger scatter seen in these data compared to Fig. 17. The data in Fig. 18 also indicate higher corrosion rates among the cylinder coupons compared to those on the coupon rack, with very high corrosion rates in the poorly drained K-South location and the highest corrosion rates among coupons on cylinder tops. However, these differences may narrow over the next sets of retrievals. Any conclusions drawn from this first set of data would be premature.

Early results from 6-month exposures of ground contact coupons are shown in Fig. 19. Again, the results are from too short a time to draw conclusions, especially with regard to the measured corrosion rates. However, it may be noted that one-sided coupons consistently showed higher corrosion losses than two-sided coupons. This supports the intuitive conclusion that ground-contact corrosion is worse than atmospheric corrosion since, for the two-sided coupons, the higher mass loss contribution from the ground contact side would be diluted by the lower mass losses from the skyward side, leading to an overall lower corrosion rate compared to ground-side-only exposed coupons.

Examination of the cylinder coupons showed that top-facing coupons were also significantly more heavily pitted than bottom-facing coupons, which may contribute to their generally higher mass losses. Figure 20 shows the results of pit depth measurements on the 1-year cylinder coupons after the corrosion product had been rinsed off. Twenty of the deepest appearing pits were measured using an optical microscope with a calibrated focussing knob, and, of these, the fifteen highest

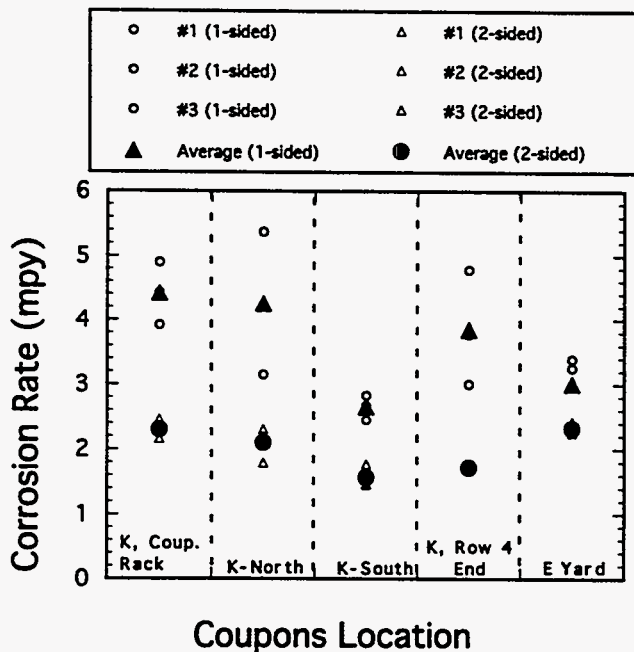
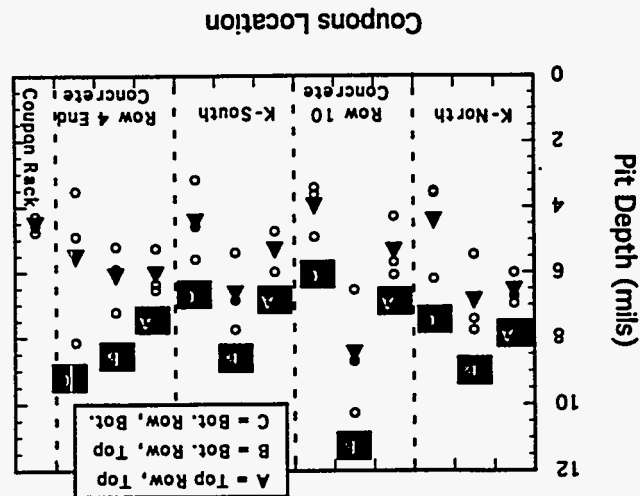


Fig. 19. Corrosion rates measured after 6-month exposure from coupons in ground contact in E and K yards. Skyward faces of one-sided coupons are protected whereas those of two-sided coupons are open to the atmosphere.

values were averaged for each data point. There is significant scatter in the data, but at each location pit depths on bottom row, bottom (BR, B) coupons are consistently lower than on the sky-facing coupons. Again it is too early to say whether pitting on bottom-facing coupons is fundamentally less or is merely delayed due to sheltering effects. Examination of two-sided ASTM G50 coupons exposed on the coupon rack for 2 years showed pits on both sides of the coupons, with no clear indication of whether the pits were deeper on any one side. This suggests that, with time, pitting on skyward faces becomes as severe as on sheltered surfaces. Unfortunately, none of the 1-year ASTM coupons were available for comparison to verify any aging effects.

Fig. 20. Results of pit depth measurements on cylinder coupons after 1-year exposure



4. DISCUSSION

There is, in general, excellent correlation between the TOW and corrosion probe data. Neither set of data showed significant effects of location. The higher initial corrosion rates observed on top-mounted probes are supported by the higher wetness times experienced by these areas. These results are probably not influenced by the heating/cooling cycles of the cylinders or their contents, since similar observations on orientation effects were made on probes mounted on coupon racks and between cylinders. Preferential dew formation on sky-facing surfaces at night appears to be the most reasonable explanation. There may be some influence of heating/cooling effects in that up-facing surfaces would cool off faster and to greater extents (as observed in the cylinder-mounted thermocouple data), leading to more condensation for longer periods of time. Due to a lack of washing action, condensed moisture has been associated with higher corrosion rates compared to precipitated moisture.^{4,21} Further aided by greater exposure to rain, the upper surfaces would therefore stay wetter longer, leading to higher corrosion rates.

It may be argued that bottom surfaces may be expected to stay damp longer due to lower evaporation and closer proximity to the ground, especially under wet ground conditions in poorly drained areas. However, TOW results clearly showed less wetness along the bottoms of cylinders even in the poorly drained pad area of K1066-K yard. As Fig. 7 demonstrated, the surfaces closest to the ground get wet only during unusually long/heavy/frequent rains. The fact that the BR, B sensors tend to have a delayed response relative to TR, T sensors indicates that moisture has to travel down the sides of the cylinders before cylinder bottoms can get wet. The overall dryness in the poorly drained area (K-South) is not easy to explain, but may be related to relatively quick absorption of pooled rainwater into the ground after rains end. The initial pooling may be caused by diversion of water from the surrounding intact concrete surfaces. Experience with similar instrumentation of UF₆ cylinders at the Paducah Gaseous Diffusion Plant has shown that cylinder bottoms there tend to stay significantly wetter, with visible near-constant dampness.²² This may be a result of significantly different ground conditions due to local rainfall, water tables, humidity, and similar factors. Not surprisingly, corrosion probes at the Paducah site also show higher corrosion rates along cylinder bottoms.

The literature shows contradictory reports on the effects of skyward (open) or sheltered surfaces on wetting response^{6,9,17,18} and atmospheric corrosion.^{7,8,12,14-16} Times-of-wetness on skyward surfaces have been reported to be sometimes more,¹⁸ sometimes less^{9,17} and sometimes both more or less⁶ than on groundward surfaces. In many cases, sheltered surfaces experienced lower corrosion rates as they were protected from the elements^{8,12,14} (as apparently in the present study), but in other cases, sheltering only served to create a more hostile "micro-environment" which increased the corrosion rates. In situations in which corrosive species tended to deposit, as perhaps in industrial environments, open surfaces benefitted from a washing action of rain leading to lower corrosion rates.⁷ However, in other examples, no clear trends were observed as corrosion rates of open specimens were sometimes higher and sometimes lower than that of sheltered specimens for multiple exposures at the same location.^{15,16} In most cases, results have been explained on the basis of specific environmental conditions existing at each test site or during the test schedule, underlining the importance of accurately characterizing the immediate environment.

The potential trends in TOW data shown in Figs. 4 (a) and (b) are difficult to explain. There is no apparent physical reason why the TR, T position at K-North appears consistently less wet than other similar positions. The explanation may lie in a lower sensitivity of this sensor compared to the

others. Although the sensors were conditioned before deployment according to ASTM recommendations for Au/Cu sensors,¹¹ no calibration tests have been performed to establish differences in response sensitivities.

One piece of data at Oak Ridge contradicts the corrosion probes and TOW data as well as the preliminary data from cylinder coupons. Visual observations and ultrasonic thickness measurements of cylinders in K-yard have shown that cylinders have experienced greater thinning near the bottoms, ostensibly due to higher corrosion rates. The greater thinning is in terms of both thinner cylinder walls (average uniform thickness) and deeper pits. This is not supported by any of the corrosion monitoring techniques. The preferential bottom thinning may be related to the effects of previous storage. The cylinders had been stored for a number of years on an asphalt surface which had badly deteriorated under the cylinders' weight, so that a large number of the cylinders were in ground contact for a number of years. Unfortunately, no tracking records exist to correlate observations with cylinder history. Cylinders in E-yard have been constantly maintained at that location and visually appear to be less corroded than those in K-yard. However, ultrasonic measurements are yet to be done on these cylinders to confirm or refute preferential bottom thinning. Thinner bottoms on K-yard cylinders cannot be reconciled with the currently available data and can only be attributed to previous poor storage conditions.

Data from the corrosion probes show initially higher corrosion rates and shorter incubation periods on open, sky-facing probes compared to bottom-facing or sheltered probes ("protected" probes). Corrosion rates on open and protected probes eventually approach similar values, and the long incubation periods of protected probes appears to be directly related to delayed wetting of such surfaces. Once wetted, corrosion rates increase and quickly approach steady-state values, as seen during the monitoring of Probe 56 described in Figs. 13 and 14. Once the corrosion product forms, corrosion proceeds at relatively high rates (Figs. 8, 9, and 13), even though neighboring TOW sensors (where present) continue to show relative dryness in these locations. Apparently, once a corrosion product forms, the corrosion process is more easily maintained, perhaps due to hygroscopic properties of the rust layer. In other words, the rust layer could be "wet" while an adjoining TOW sensor could be "dry." Apart from implying that any beneficial effects of shelter/protection is felt only as long as corrosion is not initiated, TOW measurements would tend to underestimate relative corrosion in such cases. Note, however, that the slopes of the open top-facing probes eventually decrease, leading to an overall drop in corrosion rates (Fig. 11). These data suggest that a protective corrosion product does eventually form on the probes. Data would also suggest that protected probes may also eventually show a second transition (change in slope) much like the open, top-facing probes, thus reflecting advantages of sheltered exposure. Effects of hygroscopic and other properties of rust layers on corrosion have been reported in the literature.^{4,6,7,9,12,14} In addition, as discussed below, reports of beneficial effects of sheltering often show that this exists only over relatively short time periods,^{8,12,15} as seen to date in this study.

Seasonal effects, as reflected by different corrosion rates for samples initially exposed at different times of year,^{4,7,17} were not observed in the corrosion probes data. As in the examples shown in Fig. 10, corrosion-time curves appear to be primarily influenced by the probe orientation; curve shapes and lengths of individual segments appear to be independent of the time of initial exposure. It may be noted that seasonal differences reported in the literature often disappear at long exposures.⁷ Seasonal effects, usually reflected as higher corrosion rates for winter-commenced exposures, are usually attributed to higher SO₂ levels in winter.^{4,7,17} Such situations may only be important in relatively industrial locations, quite unlike the Oak Ridge K-25 Site.

Results from the coupon corrosion program are currently insufficient to form conclusions, but by the same arguments as above, one should also expect that corrosion rates of cylinder coupons will not only be less in ensuing years, but may also reverse trends. It is generally observed that pitting corrosion is deeper and denser on rain-protected surfaces,^{4,16} the reverse of the 1-year cylinder coupon results in the present study. It will be interesting to see how the pits develop in succeeding years.

It will also be interesting to verify whether the higher corrosion rates observed on the ASTM G50 coupons in E-yard after the first 2 years of exposure will continue to be borne out in the future. This trend is not supported by any of the other monitoring techniques. Physically, E-yard is located close to a river and often tends to be fog-covered when K-yard is not. However, any excess wetness is not reflected in the TOW data. It is possible that careful analysis of the data after calibrating the sensors for relative sensitivities may establish differences.

Many of the orientation effects and preliminary trends observed in the current results and in the literature appear to be strictly valid only over relatively short exposure times, typically less than 2 years. Published data showing strong effects either have no long-term data or show narrowing differences as exposure times increase. A summary of some published observations relating to TOW and atmospheric corrosion is presented in Table 4. In five of the eight cases shown, initial differences in corrosion behavior (as a function of season, orientation etc.) evened out or reversed over longer time periods. Most of the authors reported and discussed data over relatively short time frames (three of the eight studies included only 12 months). Although this time frame may be suitable for accelerated or quick-response tests (e.g., corrosion probes), the corrosion characteristics of traditional coupon-type tests probably have not developed steady-state features. For example, results from 12-month exposures of corrosion coupons⁶ could not be correlated to factors like TOW or atmospheric pollution. Comparisons with and inferences drawn from the literature should therefore be done with care. Most experimental results are probably best explained by local criteria rather than a set of universally applicable guidelines, except in a very generalized manner.

Table 4. Published observations of atmospheric corrosion behavior as related to length of exposure

Reference	Material	Exposure time	Summary of observations
6	Cu, steel, Zn	1-12 months	Corrosion and atmospheric factors not correlated (e.g., site with highest corrosion rate of steel had relatively low time of wetness).
7	Steels	Up to 4 years	Corrosion-time curves influenced by season, but reach similar slopes (corrosion rate) at longest exposures.
8	Al, Cu, steel, Zn	3-12 months	Effects of shelter: Higher skyward corrosion rates, but differences narrow or reverse with time.
12	Steel	3-12 months	Effects of shelter/orientation: corrosion-time curves different but slopes (corrosion rate) similar after 3 months.
14	Galv. steel	1-5 years	Higher skyward mass losses throughout period.
15	Al, Cu, steel, Zn	Up to 4 years	Effects of shelter: some differences narrow or reverse by 4th year.
16	Cu, steel	1-5 years	Mixed effects of shelter; no reported time effects.
17	Zn	1-256 weeks	Short-term (seasonal) variations in corrosion rates even out over long term.

(Al = aluminum, Cu = copper, Zn = zinc.)

5. ONGOING AND FUTURE WORK

Although the corrosion monitoring program has produced significant information and data regarding the onset and progress of corrosion on the UF₆ cylinders, many issues remain and need to be addressed in FY95 and beyond. Many of these questions were raised during data analysis and interpretation which, when answered, will serve to more clearly define the direction of the corrosion monitoring program.

The critical issue in the TOW monitoring program is with regard to the relative responses of the individual sensors. At first glance, the results to date show no differences in wetting behavior as a function of yard location. However, this cannot be quantified because the relative sensitivity of each sensor's response is not known. By the same token, the magnitude of the differences seen between sky-facing and bottom-facing surfaces cannot be estimated either. To this end, each field sensor is being calibrated by exposing the sensor assemblies to controlled temperature/humidity conditions. When completed, the calibration will allow the definition of a value for the response signal voltage that corresponds to the onset of wetness. This value may be different for each sensor, as may be values for "saturation" wetness (submerged conditions) and conditions in between. Once the calibration is completed, it will be possible to conclusively examine location-to-location differences.

Other extensions to the TOW monitoring program include identification and installation of more robust relative humidity sensors as well as the incorporation of solar radiation measurements. As discussed above, there appears to be good correlation between relative humidity and TOW data. Preliminary results from weatherheads installed recently 6 inches and 6 feet off the ground at the E-yard coupon rack have shown the environmental conditions (temperature, humidity, solar radiation) to be significantly different. These results need to be confirmed and incorporated in the cylinders monitoring program by installing sensors at locations close to cylinder surfaces. These data may help recognize as-yet unidentified differences between results from yards or top and bottom cylinders.

Whereas the corrosion probes have clearly demonstrated the differences in behavior between sky-facing and bottom-facing surfaces, detailed response characteristics of an individual probe are still unclear. Metal loss versus time data appear to vary from probe to probe and may be controlled as much by the chemistry of the corrosion product formed on the surfaces as by environmental factors such as seasonal changes. Probes which have "topped out" in the measurement range (i.e., with 4 mil of nominal metal loss) will be analyzed using x-ray diffraction, electron microscopy and other appropriate analytical tools to identify the various layers of corrosion product and relate these results to probe responses over its lifetime as well as to corrosion products found on cylinders. This detailed characterization of probe response will allow clearer definition of differences in corrosion rates between locations.

Further understanding of corrosion behavior will also be provided by characterization studies of the external surfaces of the cylinders that are currently underway. The motivation for this study is that the progress of corrosion is often controlled by the nature of the corrosion products present on the surface. The goal of this project is to develop a detailed chemistry of the rust, scale, and other deposits on the cylinder surfaces and correlate these observations with existing data to anticipate future corrosion behavior. Initial results have shown the presence of lead-based paints and chromate primers, along with deposits of sulfates, presumably from "acid rain." So far chlorides have been

detected only in trace amounts. Because these contaminants significantly affect the corrosion process, interpretation of current and future data would be greatly aided by establishing the nature of the distribution of contaminants around the cylinder surfaces. For example, deep pits found on the bottoms of many of the cylinders in K-yard may be expected to be growing at accelerated rates if chlorides are present at the pit bottoms. Non-uniform pitting seen on sky-facing and bottom-facing surfaces of the 1-year cylinder coupons may be influenced by such differences in chemistry, as may be some of the observed differences in corrosion rates around the circumference of the cylinders. Similarly, these results could also aid in examining any yard-to-yard differences. Routine "chemical fingerprints" would also help identify any changes in storage conditions or the environment.

Another critical issue, not discussed in this report, is the comparison of the data presented here with similar data from monitoring programs at Paducah and Portsmouth. Preliminary comparisons have shown that whereas the data show a general similarity overall, significant differences exist. A major difference is the observation that at Paducah corrosion probes mounted on cylinder bottoms show higher corrosion rates than probes on cylinder tops; this is opposite to results from Oak Ridge. These results are supported by TOW results showing wetter cylinder bottoms—again opposite to Oak Ridge observations. One notable difference between the two sites is that at Paducah, both probes and TOW sensors are attached directly to cylinder surfaces (after removing surface rust and scale) whereas Oak Ridge uses the stainless steel strap mounting system described earlier. Strap-mounted systems have been installed at Paducah to check on possible effects of mounting geometries. Differences in data may also be related to site-to-site differences in the environment or storage conditions (e.g., Paducah is an operating plant and the UF₆ cylinder yards are downwind of active cooling towers which may affect moisture deposition on the cylinders). Data collection from the three sites through FY94 was sufficient to show that valid comparisons could be attempted. A significant effort in FY95 and future years will be directed towards making these comparisons, thus further establishing a database for drawing general conclusions about UF₆ cylinders corrosion as well as identifying parameters unique to a site.

The ultimate goal of the corrosion monitoring program is to accurately predict the remaining lifetime of the cylinders as limited by atmospheric corrosion. Ultimately, data obtained from the three sites will be used to develop a corrosion model that could be applied to predict the remaining lifetime of a UF₆ cylinder as a function of site, yard, cylinder position, age, and prior condition. Corrosion-induced cylinder breaches may well be expected to occur at the thinnest cylinder wall areas, subject to localized corrosion, in the form of pitting, galvanic corrosion, or crevice corrosion. Areas subject to these types of corrosion were identified during the initial evaluation in 1988¹, with a general conclusion that there was no overt evidence of severe localized corrosion. Pitting may occur on free surface, at inhomogeneities, around/under foreign matter or at film/coating imperfections. Expected all over the cylinder body, it may be accentuated in areas depending on specific exposure conditions. Crevice corrosion, due to local environmental differences, may occur at head/skirt interface, behind nameplates, under skip-welded stiffening rings, cylinder/chock areas and ground contact areas. Galvanic effects may occur around valves/plugs, nameplates and on cylinder bodies (due to magnetite layers or mill scale). The current program provides a good evaluation of general, uniform corrosion on cylinder bodies, but it does not address the localized corrosion issue in any great detail. Presently, it is not possible to say how fast the pits are growing or, indeed, if they are growing any faster than at the uniform atmospheric corrosion rate. The initial emphasis on monitoring cylinder body corrosion was on establishing location-to-location corrosivity differences while also addressing the excessive cylinder-bottom corrosion issue as discussed earlier. However, the programs to characterize and monitor localized corrosion will become more important in FY95 and beyond. Some work along these lines is already being done in the surface

characterization studies described above, as well as in ultrasonic wall thickness measurements on cylinder bodies that will provide baseline data for monitoring pit growth. In addition, work is planned in FY95 to ultrasonically measure wall thicknesses in cylinder heads, areas most susceptible to galvanic and crevice corrosion. This FY95 ultrasonic measuring will demonstrate the extent of or lack of a problem, and it will help establish a time frame over which to address these issues.

6. SUMMARY

An atmospheric corrosion monitoring program using TOW sensors, corrosion probes and corrosion coupons has been ongoing at the U.S. Department of Energy's Oak Ridge K-25 Site repository of UF₆ cylinders. Major results and observations to date may be summarized as follows.

1. Results from the TOW sensors and corrosion probes are in good agreement but do not completely agree with early data from the corrosion coupons.
2. Data from the TOW sensors and corrosion probes show no significant effect of cylinder yard row or stacking position. However, some TOW sensors read consistently higher or lower than others for no clear reason, and this contrast may be due to differences in sensitivities between the sensors. Early data from the corrosion coupons show possible yard and stacking differences, but it is too soon to form any conclusions.
3. Areas on top of cylinders tend to stay wetter than cylinder bottoms. This appears to be related to more dew formation on top surfaces as well as the inaccessibility of bottom areas to rain except during heavy or frequent precipitation.
4. Metal loss vs time curves from all corrosion probes show similar shapes. All probes exhibit an incubation period and a period of increased metal loss, followed by a moderation in corrosion rates in many cases, especially among top-facing probes.
5. The length of the incubation period is related to the first appearance of corrosion products and is significantly shorter on top-facing, open probes. Observations of the corroding surface support the model of atmospheric corrosion being dominant during the drying stages of an initially wet surface, at least during the early stages of corrosion product development.
6. The effects of sheltering are manifested in corrosion rates that are, at least initially, significantly higher on cylinder tops (top-facing, open probes) than bottoms (protected surfaces), an observation that is well supported by TOW data. Protection appears to delay the onset of corrosion by keeping surfaces dry, and corrosion rates on such surfaces increase once a corrosion product forms. However, there are not enough results to establish any final long-term differences in corrosion rates between the two types of exposures.
7. Corrosion probe data show no significant seasonal effects, although such effects could not be ruled out.
8. The probes and TOW data do not agree with ultrasonic measurements that have shown greater thinning and pitting on some cylinder bottoms compared to tops. This observation may be related to damage caused by prior storage in which the cylinder bottoms may have been in ground contact, leading to severe corrosion.
9. Apart from possible yard-to-yard and cylinder position differences in corrosion rates, early data from corrosion coupons also indicate a higher degree of pitting on cylinder tops. However, the data are very limited and longer exposure times are required for trends to be confirmed.

Further understanding of corrosion behavior will also be provided by characterization studies of the external surfaces of the cylinders, because the progress of corrosion is often controlled by the nature of the corrosion products present on the surface. The atmospheric corrosion monitoring program at the Oak Ridge K-25 Site is relatively young and many of the observed trends are still developing. As the corrosion database grows, more emphasis will be placed on identifying, characterizing, and monitoring areas subject to localized corrosion, including galvanic and crevice effects. Finally, A significant effort in FY95 and future years will be directed towards comparisons with similar data from the corrosion monitoring programs in the UF₆ cylinder yards at Paducah and Portsmouth. Ultimately, data obtained from the three sites will be used to develop a corrosion model that could be applied to predict the remaining lifetime of a UF₆ cylinder as a function of site, yard, cylinder position, age, and prior condition.

REFERENCES

1. Henson, H. M. et al., 1988. "Monitoring of Corrosion in ORGDP Cylinder Yards," in *Uranium Hexafluoride—Safe Handling, Processing and Transporting Conference*, Oak Ridge, TN, May 24-26, 1988, W. D. Strunk and S. G. Thornton, eds., CONF-880558-2, Oak Ridge Gaseous Diffusion Plant, pp. 103-110.
2. Henson, H. M., V. S. Newman and J. L. Frazier, 1991. "An Update on Corrosion Monitoring in Cylinder Yards," in *Second International Conference on Uranium Hexafluoride Handling*, Oak Ridge, TN, October 29-31, 1991, CONF-9110117, Oak Ridge National Laboratory, pp. 131-134.
3. UF₆ Containment and Storage Committee, 1992. *Containment and Storage of Uranium Hexafluoride at U.S. Department of Energy Uranium Enrichment Plants*, K/ETO-99, Oak Ridge K-25 Site, Oak Ridge, TN.
4. Barton, K., 1972. *Protection Against Atmospheric Corrosion*, John Wiley and Sons, New York.
5. Sereda, P. J., 1974. "Weather Factors Affecting Corrosion of Metals," in *Corrosion in Natural Environments*, ASTM STP 558, American Society for Testing and Materials, pp. 7-22.
6. Guttman, H., and P. J. Sereda, 1968. "Measurement of Atmospheric Factors affecting the Corrosion of Metals," in *Metal Corrosion in the Atmosphere*, ASTM STP 435, American Society for Testing and Materials, pp. 326-359.
7. Larrabee, C. P., 1953. "Corrosion Resistance of High-Strength Low-Alloy Steels as Influenced by Composition and Environment," *Corrosion*, v. 9, pp. 259-271.
8. Carter, J. P., P. J. Linstrom, D. R. Flinn and S. D. Cramer, 1987. "The Effects of Sheltering and Orientation on the Atmospheric Corrosion of Structural Metals," *Materials Performance*, pp. 25-32.
9. Guttman, H., 1980. "Atmospheric and Weather Factors in Corrosion Testing," in *Atmospheric Corrosion*, W.H. Ailor, ed., John Wiley and Sons, New York, pp. 51-68.
10. Sereda, P. J., S. G. Croll, and H. F. Slade, 1982. "Measurement of the Time-of-Wetness by Moisture Sensors and Their Calibration," in *Atmospheric Corrosion of Metals*, ASTM STP 767, S. W. Dean Jr., and E. C. Rhea, Eds., American Society for Testing and Materials, pp. 267-285.
11. *Standard Practice for Measurement of Time-of-Wetness on Surfaces Exposed to Wetting Conditions as in Atmospheric Corrosion Testing*, 1989, ASTM Standard G 84-89, American Society for Testing and Materials.
12. McKenzie, M., and P. R. Vassie, 1985. "Use of Weight Loss Coupons and Electrical Resistance Probes in Atmospheric Corrosion Tests," *Br. Corros. J.*, v. 20, pp. 117-124.
13. *Practice for Conducting Atmospheric Corrosion Tests on Metals*, 1989. ASTM Standard G 50, American Society for Testing and Materials.
14. Legault, R. A., and V. P. Pearson, 1978. "Kinetics of Atmospheric Corrosion of Galvanized Steel," in *Atmospheric Factors Affecting the Corrosion of Engineering Metals*, ASTM STP 646, S. K. Coburn, Ed., American Society for Testing and Materials, pp. 83-96.
15. Feliu, S., and M. Morcillo, 1980. "Atmospheric Corrosion Testing in Spain," in *Atmospheric Corrosion*, W. H. Ailor, ed., John Wiley and Sons, New York, pp. 913-921.
16. McKenzie, M., 1980. "The Corrosion Performance of Weathering Steel in Highway Bridges," in *Atmospheric Corrosion*, W. H. Ailor, ed., John Wiley and Sons, New York, pp. 717-741.
17. Guttman, H., 1968. "Effects of Atmospheric Factors on the Corrosion of Rolled Zinc," in *Metal Corrosion in the Atmosphere*, ASTM STP 435, American Society for Testing and Materials, pp. 223-239.
18. Grossman, P. R., 1978. "Investigation of Atmospheric Exposure Factors that Determine Time-of-Wetness of Outdoor Structures," in *Atmospheric Factors Affecting the Corrosion of Engineering Metals*, ASTM STP 646, S. K. Coburn, Ed., American Society for Testing and Materials, Philadelphia, pp. 5-16.

19. Hechler, J. J., et al., 1990. "A Study of Large Sets of ASTM G84 Time-of-Wetness Sensors," in *Corrosion Testing and Evaluation: Silver Anniversary Volume*, ASTM STP 1000, R. Baboian and S. W. Dean, Eds., American Society for Testing and Materials, Philadelphia, pp. 260-278.
20. Stratmann, M., K. Bohnenkamp and T. Ramachandran, 1987. "The Influence of Copper on the Atmospheric Corrosion of Iron," *Corrosion Science*, v. 27, pp. 905-926.
21. Yamasaki, R. S., H. F. Slade and P. J. Sereda, 1983. "Determination of Time-of-Wetness due to Condensed Moisture," *Durability of Building Materials*, v. 1, pp. 353-361.
22. Blue, S. C., Martin Marietta Utility Services, Paducah, KY, Private Communication.

APPENDIX A

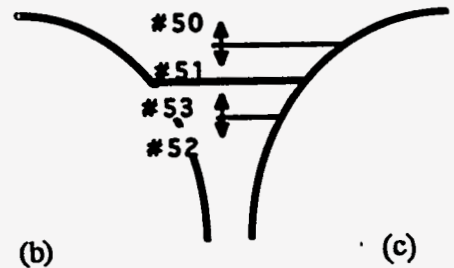
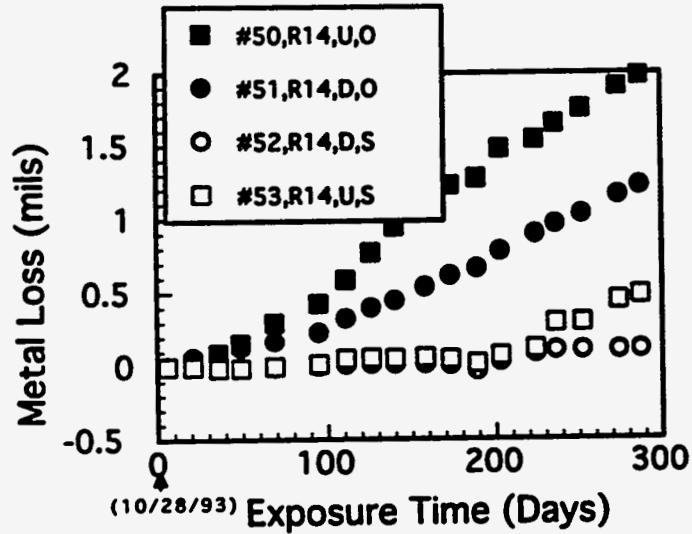
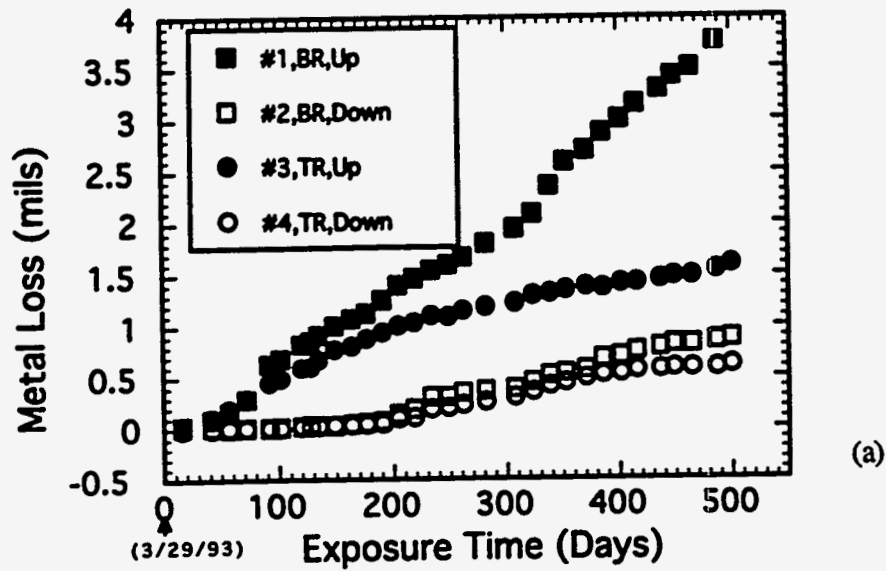


Fig. A1. Data from corrosion probes (a) 1-4 (on cylinders) and (b) 50-53 (between top row cylinders) at the K-yard North location. The sketch (c) shows the orientation of probes 50-53.

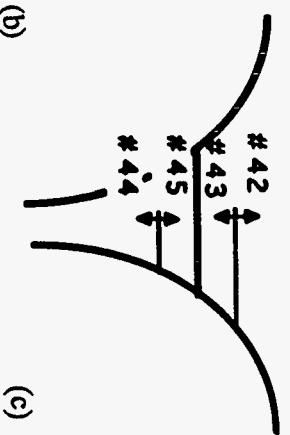
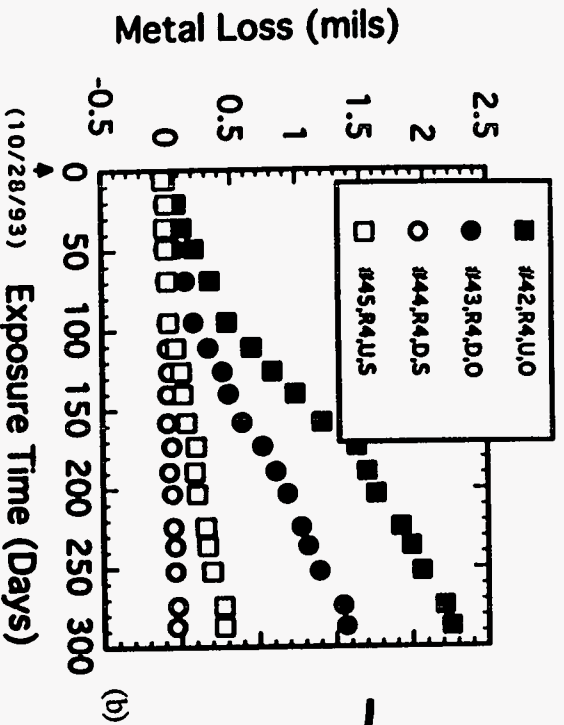
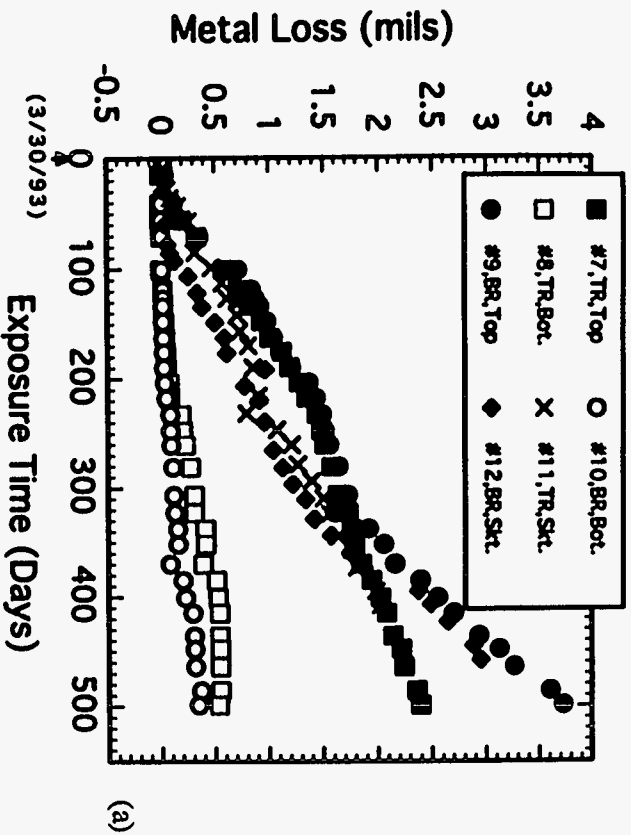


Fig. A2. Data from corrosion probes (a) 7-12 (on cylinders) and (b) 42-45 (between top row cylinders) at the K-yard South location. The sketch (c) shows the orientation of probes 42-45.

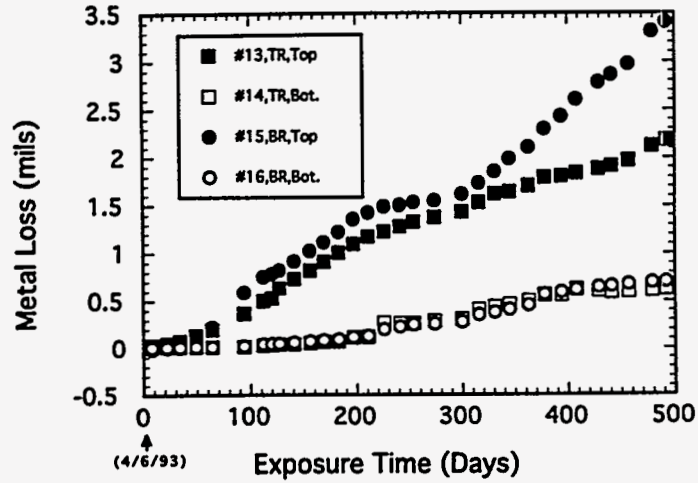


Fig. A3. Data from corrosion probes 13–16 on cylinders at the E-yard location.

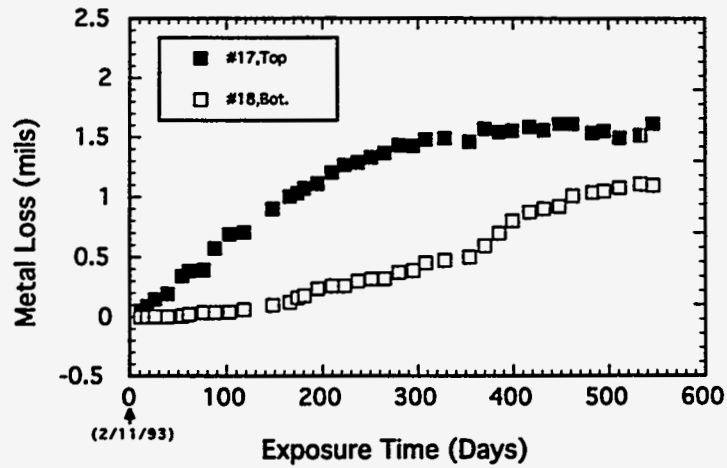


Fig. A4. Data from corrosion probes 17 and 18 on a new cylinder at the entrance to E-yard.

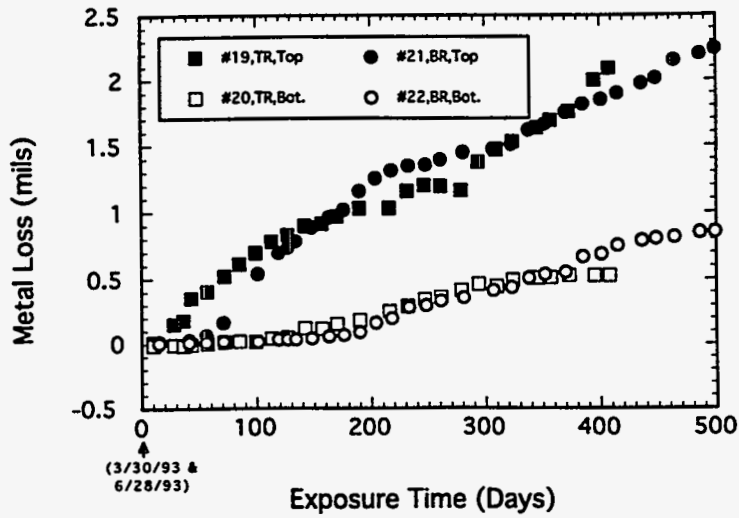


Fig. A5. Data from corrosion probes 19–22 on relatively heavily corroded TR and BR cylinders in K yard, row 10, concrete pad.

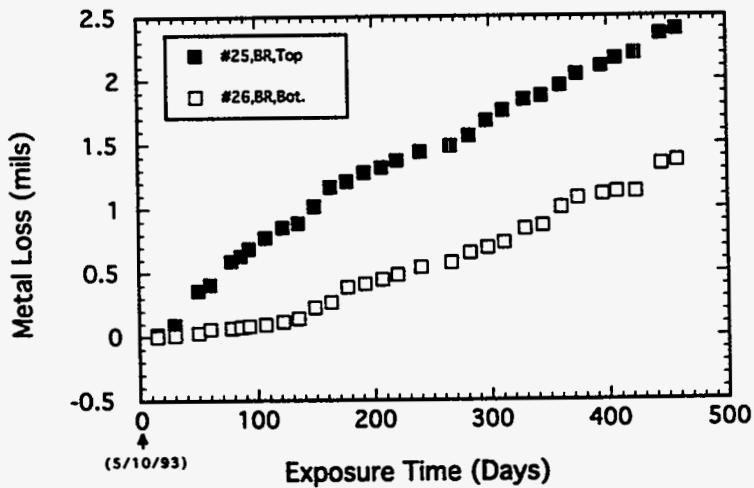


Fig. A6. Data from corrosion probes 25 and 26 on a relatively lightly corroded BR cylinder in K yard, row 14, gravel pad.

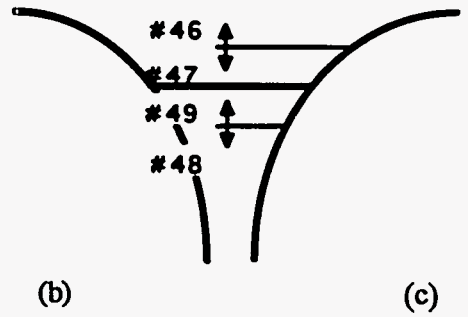
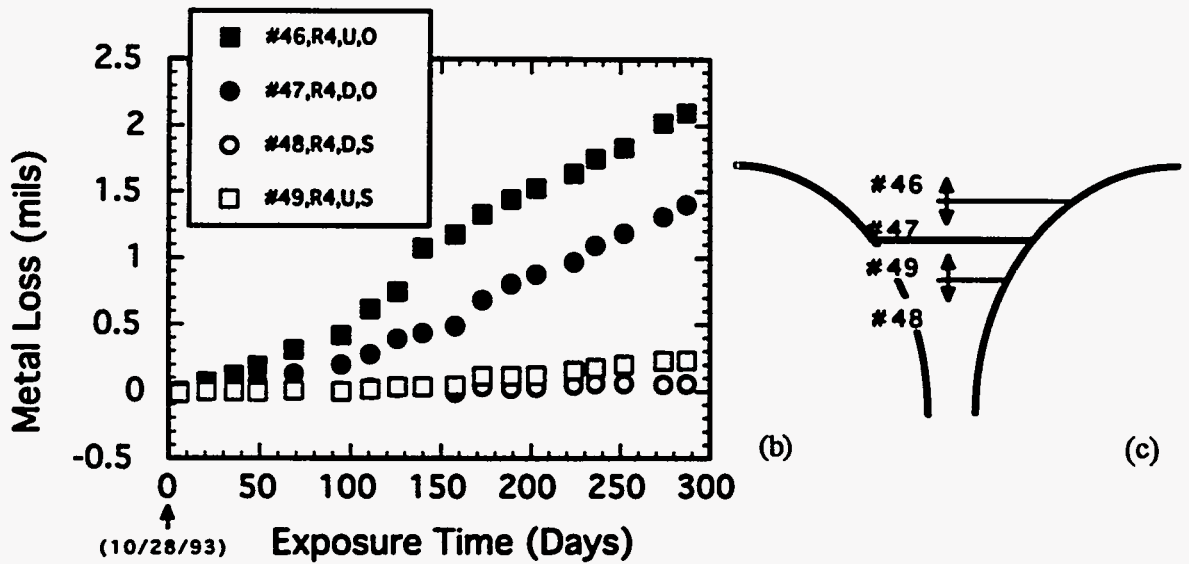
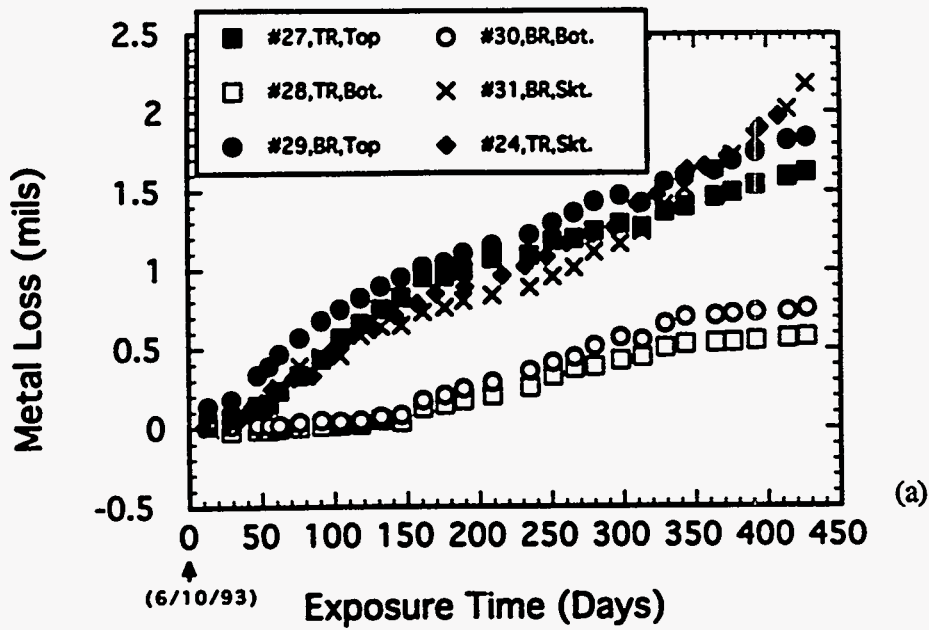


Fig. A7. Data from corrosion probes (a) 24, 27-31 (on cylinders) and (b) 46-49 (between top row cylinders) on relatively lightly corroded cylinders in K-yard, row 4, concrete pad. The sketch (c) shows the orientation of probes 46-49.

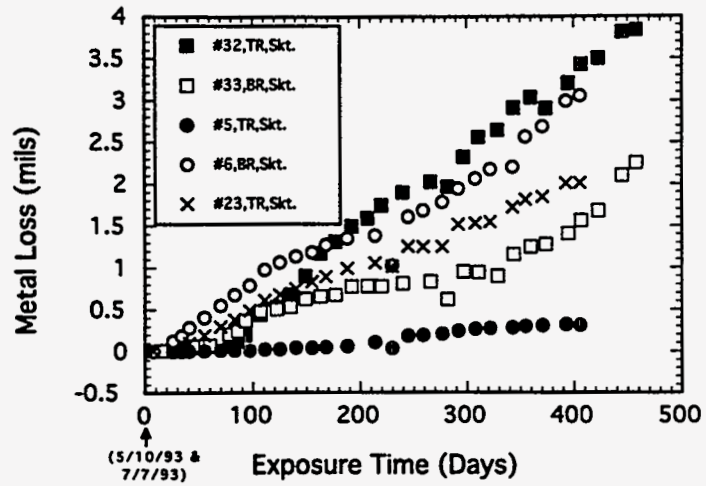


Fig. A8. Data from corrosion probes 5, 6, 23, and 33 on relatively heavily corroded TR and BR cylinders in K-yard, row 3, concrete pad.